Annex 54-1

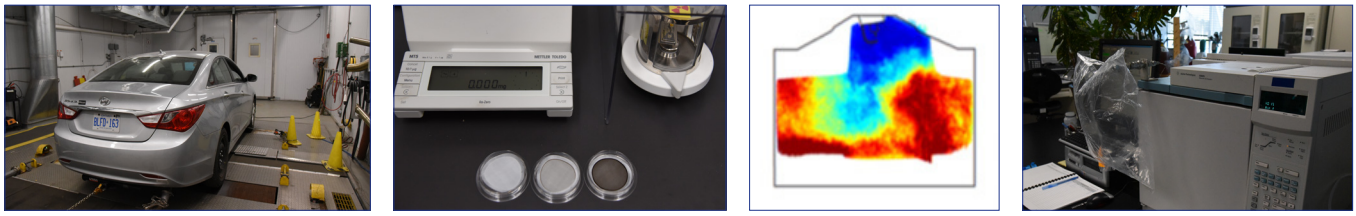

A Report from the Advanced Motor Fuels Technology Collaboration Programme

GDI Engines and Alcohol Fuels

Debbie Rosenblatt
Environment and Climate Change Canada

Deniz Karman
Professor Emeritus, Carleton University

IEA-AMF ADVANCED MOTOR FUELS
Technology Collaboration Programme on
Advanced Motor Fuels

Technology Collaboration Programme
by iea

Annex 54-1

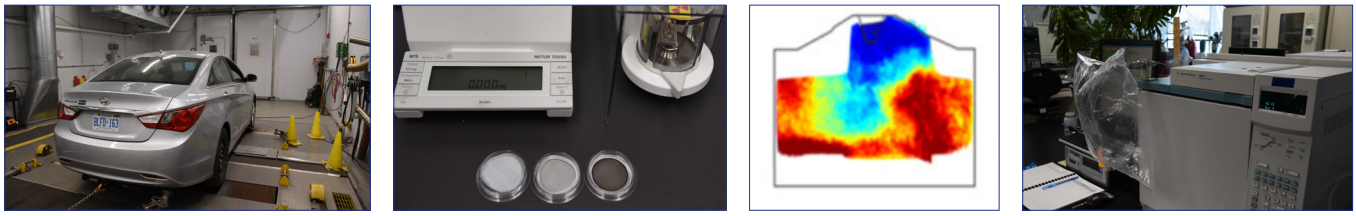

A Report from the Advanced Motor Fuels Technology Collaboration Programme

GDI Engines and Alcohol Fuels

Debbie Rosenblatt
Environment and Climate Change Canada

Deniz Karman
Professor Emeritus, Carleton University

ADVANCED MOTOR FUELS
IEA-AMF
Technology Collaboration Programme on
Advanced Motor Fuels

February 2020

Technology Collaboration Programme
by iea

Summary / Abstract

This report is based on research carried out in five participating countries (Canada, Germany, Israel, Switzerland, United States) participating in the Advanced Motor Fuels Technology Collaboration Programme of the International Energy Agency during 2016-2019. Gasoline Direct Injection (GDI) technology is generally considered an effective means of reducing fuel consumption and emissions although GDI engines emit a higher number of particles than Port Fuel Injection (PFI) engines. Alcohol blended gasoline used in vehicles with spark ignition engines also have generally favorable effects on the emissions from these vehicles. The objective of IEA-AMF Annex 54 is thus to determine the impacts of alcohol fuels on emissions from GDI engines.

The work reported for Annex 54 by the participating countries covers a relatively wide range of specific issues and research methodologies, from studies on pollutant formation within a single cylinder engine to the simulation of the behaviour of emissions once they are in the atmosphere, with the measurement and characterization of emissions at the tailpipe of vehicles being a central concern. The report therefore discusses results in three broad categories: Combustion and Pollutant Formation; Tailpipe Emissions; and Secondary Organic Aerosol Formation and Genotoxic Potential of emissions. The effects of alcohol fuel blends on pollutant formation, tailpipe emissions, secondary aerosol formation, and the genotoxicity of emissions are addressed. Gasoline particulate filters (GPF) are emerging as the technology to ensure conformance with regulations on particulate matter emissions from light duty vehicles measured on the basis of number of particles emitted per distance travelled. The effectiveness of GPFs in reducing particulate matter emissions as well as their impact on the secondary aerosol formation potential and the genotoxicity of emissions are among the subjects addressed by some of the studies. A trend that is emerging alongside the increase of GDI technology in light duty vehicles is the "start-stop" operation technology that enables the engine to shut off when stopped for more than a short period and to re-start automatically when the driver ends the stopping action. The main purpose of the technology is to save fuel that would otherwise be wasted as the engine idled while the vehicle was stopped. While carbon dioxide emissions are directly proportional to the fuel used (or saved), the effect of such start-stop operation is of interest from the perspective of the emission of other pollutants in the exhaust.

Authors

The studies and reports submitted under Annex 54 were carried out and authored by numerous researchers as indicated below. A publication by Gramsch et al (2017) is also reviewed in various sections of this report.

Canada

Fadi Araji
Jonathan Stokes

Germany

Michael Storch
Matthias Koegl
Michael Wensing
Stefan Will
Lars Zigan

Israel

Gideon Goldwine
Eran Sher

Switzerland

P. Comte,
J. Czerwinski
A. Keller
N. Kumar
M. Muñoz
S. Pieber
A. Prévôt
A. Wichser
N. Heeb

United States

John M. Storey
Melanie Moses-DeBusk
Shean Huff
John Thomas
Mary Eibl
Faustine Li

Contents

Abbreviations

AMS	Aerosol Mass Spectrometer
BC	Black Carbon
c-	cold, catalyzed (based on context)
cat-	catalyzed
° CA	Crank angle degrees
	aTDC after Top Dead Centre, bTDC before Top Dead Centre
CMOS	complementary metal oxide semiconductor
CPC	Condensation Particle Counter
CVS	Constant Volume Sampling system
DMA	Differential Mobility Analyzer
DPF	Diesel Particulate Filter
eBC	Equivalent Black Carbon (determined by Aethalometer)
EDC	European Driving Cycle
EEPS™	Engine Exhaust Particle Sizer
ELPI	Electrical Low Pressure Impactor
FID	Flame Ionization Detector
FTP, FTP-75	United States Federal Test Procedure
GC-HRMS	Gas Chromatography High-Resolution Mass Spectrometry
GDI	Gasoline Direct Injection
GPF	Gasoline Particle Filter
h-	hot
iB16, iBu12	16%, 12% isobutanol in gasoline blend
LED	Light Emitting Diode
nanoSMPS	Nano Scanning Mobility Particle Sizer
NEDC	New European Driving Cycle
	(consisting of urban UDC, and extra-urban EUDC phases.)
NMHC	Non-Methane Hydrocarbons, (determined by FID)
nc-	non-catalytic
OEM	Original Equipment Manufacturer
OFR	Oxidation flow reactor (a potential aerosol mass, PAM, reactor)
PAH	Polycyclic Aromatic Hydrocarbons
PN	Particle Number
POA	Primary Organic Aerosol
PTR-ToF-MS	Proton Transfer Reaction Time-of-flight Mass Spectrometer
RON95	Research Octane Number rating of 95
SC	Smog Chamber
SMPS	Scanning Mobility Particle Sizer
SOA	Secondary Organic Aerosol
SSC	Steady State Cycle
TEM	Transmission Electron Microscopy
TWC	Three Way Catalyst
WLTC	World Harmonized Light Vehicle Test Cycle

1. Introduction

1.1 Context and Participants

This report is based on research completed in six countries participating in Annex 54: GDI Engines and Alcohol Fuels, under the Technology Collaboration Programme on Advanced Motor Fuels, of the International Energy Agency.

The institutional representation of the participating countries and the reports/publications submitted for the preparation of the Annex 54 report are as follows:

- **Canada** (Araji & Stokes 2019)
  - Emissions Research and Measurement Section (ERMS) of Environment and Climate Change Canada
- **Germany** (Annex A)
  - Institute of Engineering Thermodynamics (LTT) at Friedrich-Alexander-Universität Erlangen-Nürnberg (FAU)
- **Israel** (Annex B)
  - Technion – Israel Institute of Technology (experimental work was conducted at the vehicle emission laboratory (VELA) of the Joint Research Centre of the European Commission (JRC) located in Ispra, Italy)
- **Switzerland** (AFHB 2016, Empa 2017)
  - Paul Scherrer Institute (PSI)
  - University of Applied Sciences Northwestern Switzerland (UASNW)
  - University of Applied Sciences Bern (UASB)
  - Swiss Federal Laboratories for Materials Science and Technology (Empa)
- **United States** (Storey et al 2019)
  - Oak Ridge National Laboratories (ORNL) with the U.S. Department of Energy

Although Chile was not formally a participant in the Annex 54 program, published work (Gramsch et al 2017) carried under auspices of the 3CV laboratories in Chile contain relevant findings for this report and excerpts from the publication have been included under Chile subheadings in the appropriate sections.

1.2 Annex 54 objectives, structure of report

The objective of Annex 54 under the Advanced Motor Fuels programme is to determine the impacts of alcohol fuels on emissions from GDI engines. In addition to gaseous emissions, the interest is on the tailpipe emissions of PM and black carbon (BC), along with the secondary organic aerosol (SOA) formation potential. The fuels investigated include ethanol, methanol and isobutanol, and their blends with gasoline. The impacts of gasoline particulate filters

(GPFs) on emissions from gasoline direct injection (GDI) engines with varying fuels are also investigated.

The work reported for Annex 54 by the participating countries covers a relatively wide range of specific issues and research methodologies. Most studies are based on chassis dynamometer tests of vehicles with GDI engines and comparable counterpart engines, focusing on tailpipe emissions, especially particulate matter emissions, under different driving cycles and the use of different fuel blends. The contribution from Germany looks at the fundamental processes of combustion and pollutant formation in a unique single cylinder engine, while the contribution from Switzerland document s original experimental and modelling approaches to addressing the secondary organic aerosol formation potential of GDI emissions and the genotoxicity of GDI vehicle emissions. Section 2 of the current report thus presents an overview of the completed studies under three categories: Combustion and Pollutant Formation; Tailpipe Emissions; and Secondary Organic Aerosol Formation and Genotoxic Potential of emissions, making connections between these categories and their implications.

In the remainder of this introductory section the motivation for and the current status of GDI vehicles and alcohol fuels are briefly reviewed.

Section 3 summarizes the key findings of the studies in terms of the overall objectives of the Advanced Motor Fuels Technology Collaboration Programme.

The content presented in various subsections of Section 2 have been distilled mostly from reports or journal articles that are now publicly available. In the case of contributions from Germany and Israel, reports designated specifically for input to the Annex 54 report were received and have been included as Annex A and B respectively.

1.3 Motivation for and status of GDI and alcohol fuels

Concerns with energy efficiency and the environmental effects of road vehicles have historically been addressed by alternately focusing on the engines, the fuels, and exhaust after-treatment devices although these three elements can rarely be designed and optimized individually (Sawyer 1992). Engine design is constrained by the fuel available, gasoline and diesel fuel are produced to meet the requirements of the engine that will burn them, after-treatment technologies are dependent on fuel and engine operating characteristics (Chevron 2011). The interdependence of these elements have become stronger as improvements in each have been sought to meet increasingly tighter emission regulations, resulting in a complex system of sensors and electronically controlled elements coordinated by a computer for the functioning of an engine. Gasoline direct Injection and the renewed emphasis on ethanol (and other alcohols) can be considered one of the more recent developments in this history.

Ethanol was originally considered an oxygenated fuel additive for octane enhancement and "cleaner combustion" i.e. its beneficial effects on tailpipe emissions. The importance of the latter role was somewhat diminished with the aggressive after-treatment systems that became

necessary to meet the increasingly tighter emission regulations, irrespective of the fuel being used. The interest in biofuels for their potential to reduce CO_2 emissions in transportation has resulted in an increased role played by ethanol even though the life-cycle studies of ethanol production pathways are not particularly promising for net reductions. Nevertheless, ethanol mandates for gasoline have increased fuel ethanol in the United States from 6.5 billion gallons in 2007 to 15.8 billion gallons in 2017[1]. Worldwide, ethanol production for fuel use went from 66.8 million cubic meters in 2008 to 98.9 million cubic meters in 2017[2]. In the present context, the effect of ethanol blends on particulate matter formation in GDI engines has been the subject of recent studies with findings pointing to reductions relative to unblended gasoline (IEA-AMF 2105, Munoz et al 2016, Gramsch et al 2017). Other alcohols, although not currently used at any significant scale, have also attracted attention for the evaluation of their potential. For example butanol blends have been part of the testing along with ethanol blends in three out of the six country submissions for the compilation of this report. Karavalakis et al (2018) review the literature addressing fuel effects on PM emissions which show complex relationships among fuel as well as driving parameters.

GDI technology is generally considered an effective means of reducing fuel consumption and emissions on the one hand and greatly boosting driving dynamics on the other. Combined with innovative downsizing concepts and turbocharging, it is estimated that reductions in fuel consumption and CO_2 emissions can be delivered in the region of 15%.[3] GDI engines have been increasing in the light duty fleet in the United States, reaching 52% of all new cars and light trucks in 2017 (EPA 2018).

In the Introduction section of their manuscripts Yang et al (2018) provide a comprehensive review of the basic technology and status of GDI vehicles, highlighting the pollutant formation mechanisms at play that give rise to higher particulate matter emissions from GDI engines compared to traditional port fuel injection engines. They also provide a review of the evolution of particulate mass and particle number emission regulations in the US and Europe respectively that pose challenges for GDI vehicles and discuss developments in gasoline particulate filter and alternate fuel arrangements being considered to meet these challenges. A recent review (Raza et al 2018) focuses on the particle number emissions and their control techniques. In a previous publication Czerwinski et al (2016 & 2017) present experimental data on five GDI vehicles and demonstrate the effectiveness of the GPFs for these vehicles in reducing particle number emissions below future regulatory limits.

---

[1] RFA, Renewable Fuels Association, 2018. "Ethanol Strong: 2018 Ethanol Industry Outlook". http://www.ethanolresponse.com/wp-content/uploads/2018/02/2018-RFA-Ethanol-Industry-Outlook.pdf (accessed 20 November 2018)

[2] Global ethanol production for fuel use from 2000 to 2017. https://www.statista.com/statistics/274142/global-ethanol-production-since-2000/ (Accessed 20 November 2018)

[3] Gasoline direct injection – Key technology for greater efficiency and dynamics http://www.bosch.co.jp/tms2015/en/products/pdf/Bosch_di_folder.pdf (Accessed 22 November 2018)

Emissions of particulate matter from vehicles have been the subject of regulations on the basis of either mass or number emitted per distance travelled. Although the chemical composition is not readily determined and thus not the subject of regulation, it clearly has significance from the perspective of human health effects when these particles are inhaled. Components of vehicle exhaust other than the measured particulate matter, i.e. gaseous components, have the potential to form secondary particulate matter in the atmosphere after being emitted from the tailpipe of the vehicle. This secondary aerosol forming potential of vehicle exhaust represents potential human health effects and has received increased attention in related research. Thus, the genotoxicity of tailpipe emissions and their secondary organic aerosol formation potential are among subjects addressed by some of the reports summarized in later sections of the current report. In a previous publication Munoz et al (2016) address these chemical effects in connection with the use of bioethanol blends in a flex-fuel GDI vehicle. Pieber et al (2018) address the complex issue of SOA formation potential of particle filter retrofitted GDI vehicle exhaust emissions.

The role that can be played by gasoline particulate filters and alcohol fuels has been directly the focus of some country contributions to Annex 54 as will be detailed in later sections of the report (AFHB 2016, Empa 2017, Araji & Stokes, 2019). A previous report prepared for the IEA AMF program under Annex 35-2 is discussed in the next section.

1.4 Previous related work under IEA –AMF Annex 35-2

(Excerpts from IEA-AMF 2015)

Previous research completed under IEA-AMF Annex 35-2 can be considered a precursor to the work being reported under Annex 54 in this report. Work under *Annex 35: Ethanol as Motor Fuel – Subtask 2: Particulate Measurements: Ethanol and Butanol in DISI Engines* was carried out as an international collaborative study, the overall program involving the following components:

North American Test Program:

Canada

Emissions Research and Measurement Section (ERMS) of Environment and Climate Change Canada performed chassis dynamometer emissions testing of a flex-fuel GDI vehicle and a standard GDI vehicle over a variety of fuel, drive cycle and temperature configurations. Real-time continuous monitoring using an EEPS determined particle size and number emission rates.

Through the Auto21 Network (Universities of Alberta, British Columbia and Toronto) SMPS scans were performed using a combination of a 3081 series DMA and a 3776 series CPC to assess particle size and number emission rates from a GDI engine tested on an engine dynamometer. Primary particle morphology was investigated with a TEM.

United States

Argonne National Laboratory (ANL) used engine dynamometer testing to study particulate emissions from a General Motors GDI engine operating on alcohol blended fuels at different load levels. Particle size and number were determined with a SMPS and soot morphology was analyzed by TEM.

European Test Program:

Finland

VTT Technical Research Centre of Finland conducted chassis dynamometer emissions testing on a turbocharged, direct injection, spark ignited engine run on 85% ethanol fuel using the NEDC. Particle size distributions were assessed by an ELPI.

The final report from Annex 35-2 (IEA-AMF 2015) summarized particulate data from two different GDI engines and three different GDI vehicles tested in four separate facilities in three countries. These engines and vehicles were tested under different operating modes, driving conditions, and at different ambient test conditions to assess the impacts of alcohol fuel blends and varying fuel blend levels on particulate emissions.

The use of low- to mid-level alcohol blends (E10, E15, E20, iB16) with these GDI engines/vehicles gave mixed results; with some studies noting decreases in particles with alcohol blends and some studies showing increases. These test alcohol fuels were splash blended with gasoline and an investigation of the impacts of other fuel parameters, besides alcohol content, on emissions was not undertaken.

In contrast to the low level ethanol blends the E85 studies did yield consistent results indicating the potential to mitigate particulate emissions from GDI engines. Research conducted with two test engines under the North American program and one vehicle under the European test program using E85 as a test fuel showed that reductions in particle emissions from GDI engines can be achieved under varying operating conditions and ambient temperatures. In some cases the number of particles was roughly an order of magnitude lower with E85 as compared to E10 and resulted in reductions in the range of 70–90% between E85 and E0. Along with a reduction in particle number, the shape of the particle number distribution curve was also impacted with the distribution peak occurring at a smaller particle size with E85 compared to E10 and E0.

2. Research Methodologies and Results

With the exception of the report from Germany which is focused on combustion fundamentals in an optically accessible single cylinder engine, the reports from all the other participants have included results from chassis dynamometer testing procedures and driving cycles for light duty vehicles. A comparative summary of the tests employed in the individual reports is therefore informative of the body of work presented. The organization of Table 1 is guided by the characteristics of chassis dynamometer tests on vehicles but also includes, for the sake of completeness, the single cylinder investigation reported from Germany, and the parts of contributions that deal with the after effects of tailpipe emissions measured by chassis dynamometer tests, such as secondary aerosol formation, and the genotoxicity of emissions. This section will address the basic issues related to the investigations in three related but distinct categories: the nature of combustion and pollutant formation processes in gasoline direct injection engines (Section 2.1), the emissions measured at the tailpipe of vehicles (Section 2.2), and the human health/environmental effects of these emissions (Section 2.3).

Table 1. Summary parameters from studies for Annex 54 reporting

Study	Vehicle(s)/Engine(s)	Fuel(s)	Aftertreatment	Tests	Measurements
Canada	3 vehicles: PFI_1 GDI_1 GDI_2	gasoline	nc-GPF c-GPF	25 and -7C FTP-75 US06 PEMS	CO2 ,CO, NOx, THC PM (particle mass, Gravimetric Sampling) BC (black carbon, laser-induced incandescence) PN (particle number and size distribution, Electrical Mobility Classification)
Chile*	2 vehicles Ford Focus 2.0 GDI Chevrolet Prisma 1.4 flex-fuel	E0, E10, (E85S, E75W) E22, E100	TWC TWC	25 C 2 X FTP 3 X NEDC cold and hot start (UDC, EUDC phases) Photochemical chamber	THC, NMHC, CO, NO_x , CO_2. NO, NO_y, O_3 , PM (deduced from SMPS data)
Germany	Single cylinder optical accessible DISI engine 1.8 L turbocharged 4-cylinder DI engine	Ethanol, Isooctane, E20 (20% ethanol 80% isooctane) Gasoline (RON 98), E20	Not applicable	Steady state operating points	In-cylinder: OH radical chemiluminescense, soot luminosity, laser induced fluorescence (LIF) Exhaust: laser-induced incandescence (LII) soot sensor
Israel	3 vehicles: GDI, turbocharged GDI, PFI	E85, RON95, M56	TWC	22 C NEDC	CO, CO_2, NOx, HC, NMHC; Particulate Mass (PM), Particle Number (PN); formaldehyde (pre- and post TWC)

* Although Chile was not formally a participant in the Annex 54 program, published work (Gramsch et al 2017) carried under auspices of the 3CV laboratories in Chile contain relevant findings for this report and excerpts from the publication have been included under Chile subheadings in the appropriate sections.

Table 1. Summary parameters from studies for Annex 54 reporting (continued)					
Study	**Vehicle(s)/Engine(s)**	**Fuel(s)**	**Aftertreatment**	**Tests**	**Measurements**
Switzerland	7 GDI vehicles (Euro 3-6) 1 Diesel Euro-5 vehicle	Gasoline, blends with ethanol (E0, E10, E85) and butanol diesel	Gasoline Particulate filters DPF	WLTC (city, urban, cold, hot); EDC (cold and hot); SSC (urban, extra-urban, highway, motorway and idle) smog chamber (SC), potential aerosol mass oxidation flow reactor (PAM-OFR), micro smog chamber (MSC)	4 work packages (WP) at different laboratories: WP 1: regulated pollutants ; WP 2: nanoparticles; WP 3: secondary organic aerosols; WP 4: non-regulated pollutants and metals Particle size distribution, number and metal content Comparison of the particle burden, the genotoxic potential and the SOA formation potential of GDI and diesel vehicles.
United States	2014 Chevrolet Malibu Eco equipped with a 2.5L GDI engine and start-stop operation	Base fuel: 87 AKI gasoline; E21 (21% ethanol blend in the base fuel); iBu12 (12% isobutanol blend in base fuel)	TWC	FTP-75, With and without start-stop operation	CO, CO_2 , NOx, and HC PM (filter), PN (EEPS) Soot mass (AVL MSS)

Vehicles: DI, GDI (Gasoline) Direct Injection; **PFI** Port Fuel Injection; **LDV** Light Duty Vehicle; **DISI** Direct Injection Spark Ignition;
Aftertreatment: nc-GPF non-catalyzed Gasoline Particulate Filter; **c-GPF** catalyzed Gasoline Particulate Filter; **TWC** Three Way Catalyst; **DPF** Diesel Particulate Filter
Tests: FTP-75 United States Federal Test Procedure; **US06** Supplemental Federal Test Procedure; **PEMS** Portable Emission Measurement System for on-road measurement; **EDC**, **NEDC (**New) European Driving Cycle (urban UDC, extra urban EUDC phases); **WLTC** Worldwide harmonized Light vehicle Test Cycle; **SSC** Steady State Cycle .
Measurements: EEPS Engine Exhaust Particle Sizer; **AVL MSS** photoacoustic-based Micro Soot Sensor™ (MSS, AVL Model 48

2.1 Combustion and Pollutant formation in a GDI engine

Germany

(Excerpts from Annex A and related references)

The contribution by Germany to the Annex 54 related work contains fundamental investigations of mixture formation and soot formation in an optically accessible single cylinder engine using a powerful array of measurement and visualization methods. Further characterizations of PM were conducted in the exhaust gas duct of a metal GDI engine equipped with a GPF.

The IC engine experiments mentioned above were conducted in a framework of interdisciplinary research program that also included the study of particle formation in laboratory scale flames, IC engine simulations of soot formation and oxidation, and, the development of a highly efficient catalyst for the rapid oxidation of soot in particle filters. The summary report from Germany is included in its entirety as Annex A. It provides details of the institutions involved in the overall research program and includes references to some 17 published articles providing details on the work completed.

2.1.1 Experimental setup

Single cylinder optical access engine

The measurements were performed in an optically accessible single cylinder engine based on a modified BMW/PSA series-production engine ("Prince") with direct injection. The engine is equipped with a variable valve train and lateral position of the injector (BOSCH, solenoid, 7-hole).

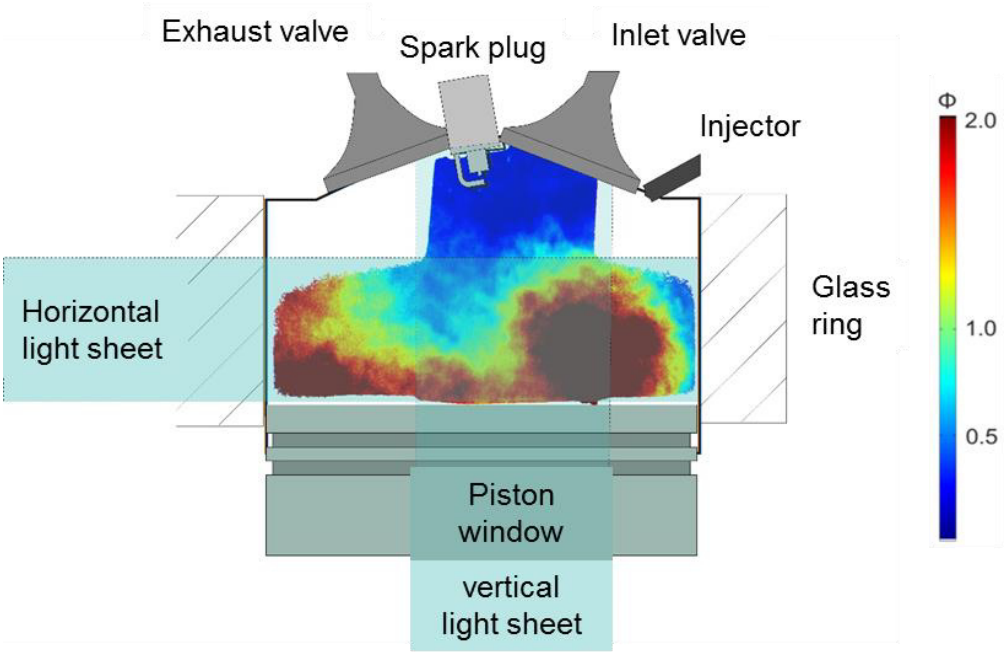

Optically accessible IC engine cylinder with horizontal and vertical laser light sheet. The camera field of view contains an example image of the mixture formation (FAR, ϕ) obtained by overlapping two laser light sheets (Annex A, Figure 2)

Planar laser-induced fluorescence (LIF) (Storch et al 2016) was used to observe fuel-air mixing in the cylinder, clarify the effects of biofuel blends on mixture formation and the resulting sooting combustion. By visualizing fuel rich zones, potential sources of soot formation could be identified and correlated with measured PM emissions.

Fuels and operating conditions

Different fuels were used in the single cylinder engine to study fuel effects in soot formation, with isooctane used as the surrogate fuel in the blends. The fuels for the single cylinder optical access engine thus included:

- Isooctane
- Pure ethanol
- n-butanol
- E20 and E85 (20%, and 85% ethanol blend with isooctane)
- "Toliso" (35% toluene, 65% isooctane blend)

The investigated operating points for the engine are representative of part load conditions at different injection timings (i.e. different start of injection (SOI)). Characteristic engine operating points were selected, which represent typical driving situations in order to study fuel effects and mechanisms of soot formation. The specifications of the investigated operating points are presented in the table below.

(Annex A, Table 1) Specifications of the studied operating points for iso-octane.

Operating Point	unit	Base Point	Late Injection	Globally fuel rich	Catalyst heating: Inhomogeneous mixture	Catalyst heating: poolfire
Engine speed	U/min	1500	1500	1500	1200	1200
Air mass flow	kg/h	6.3	6.5	6.3	4.8	5.5
Global air fuel ratio λ	-	1	1	0.75	1	1
IMEP	bar	2.7	1.2	2.6	1.8	2.2
Rail pressure	bar	70	70	70	70	70
Injection time (SOI1/SOI2)	°CA bTDC	300/-	145/-	300/-	300/73	300/50
Injection duration (SOI1/SOI2)	ms	1.25	1.2	1.8	0.94/0.24	0.78/0.48
Spark timing	°CA bTDC	28	28	28	0	0

The "Base Point" refers to an early fuel injection leading to a homogeneous stoichiometric fuel-air mixture. Similar IC engine parameters were used for the Operating Point "Globally fuel rich

mixture", mainly the global relative air-fuel ratio (λ) was adjusted to 0.75 (or an equivalence ratio Φ of 1.33). The other operating points refer to late injections or split injections, which are usually applied for heating of the catalyst during cold start operation. For a very late second injection, the fuel wall wetting is observed leading to sooting pool fires.

2.1.2 Results

In-cylinder Mixture Formation Results

An example of the fuel-air mixing observations in the cylinder is presented in the following figure for the "Late Injection" operating point at three stages in the movement of the piston in the cylinder. Overall, the mixture distribution for all fuels at later times appears very similar in structure. Very fuel-rich zones are visible near the piston and a "tumble flow" is formed during compression, so that a larger vortex with a fuel-rich mixture is transported towards the spark plug. At later points in time, this mixture stratification is reduced, while larger inhomogeneities and richer zones exist especially for iso-octane and E20 (see for example 48°CA BTDC). These locally fuel-rich zones of E20 and iso-octane can explain the significantly larger PM concentration in the exhaust gas for these two fuels compared to E85 and pure ethanol (see below in Figure 4 from Annex A). In these fuel-rich zones, sooting combustion was also identified in soot luminescence measurements (Storch et al 2014). Further details of the mixture formation study and results for further operating points are found in (Storch et al 2015, and Storch et al 2016).

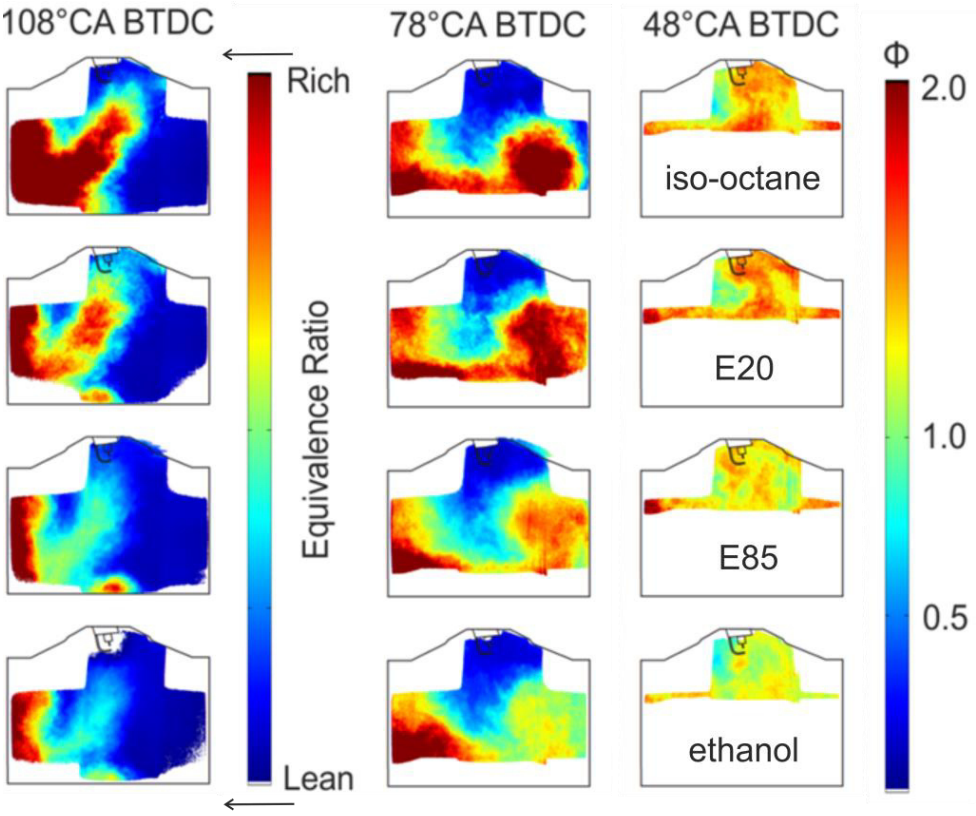

Distribution of fuel-air ratio for OP "Late injection" for iso-octane (top row), E20 (row 2), E85 (row 3) and pure ethanol (bottom row) (Annex A, Figure 3) (Storch et al 2016)

Exhaust measurement of PM

Exhaust primary particle concentrations were measured with a laser-induced incandescence (LII) sensor developed at LTT and placed in the engine exhaust duct, capable of measuring carbon particle concentration in the range of 0.001–200 mg/m^3. The observations over a 90 s run were averaged to report for each operating point. The PM measurements for the operating points and different fuels cited above are directly relevant for the effect of alcohol blends on PM emissions from DI engines and are therefore discussed in Section *2.2.1.2 Effect of alcohol fuel blends on particle emissions*

In-cylinder Soot formation and Oxidation Investigation

The optical test setup for soot volume fraction measurement consists of a high-speed CMOS camera and a LED panel for illumination of the soot cloud in the cylinder. In principle, the time-resolved detection of soot radiation as well as the light extinction is possible by using a stereoscope with two different filters, and in fact there is good agreement between the shape of the soot clouds observed with the two techniques. As the soot cools down during the downstroke the signal of soot radiation gets much weaker than the light extinction signal. Thus, only the light extinction method was used for further quantitative analysis. Further details can be found in (Koegl et al 2018, Koegl et al 2019)

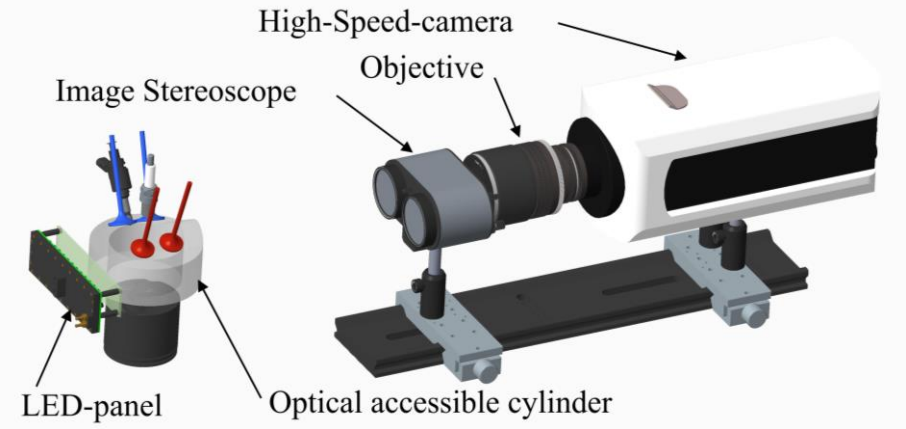

Optical setup for combined high-speed light extinction and soot luminescence measurements (Annex A, Figure 6)

Examples of in-cylinder cloud images that can be obtained with the light extinction technique are shown in the next figure for one cycle of one of the operating points (OP2). The soot distribution and the change in its concentration is clear from the intensity of the extinction signal which is provided in terms of the extinction *KL*, which is the product of the path length in the probe volume *L* and the average extinction coefficient *K* (further details are provided in Koegl et al 2018, Koegl et al 2019).

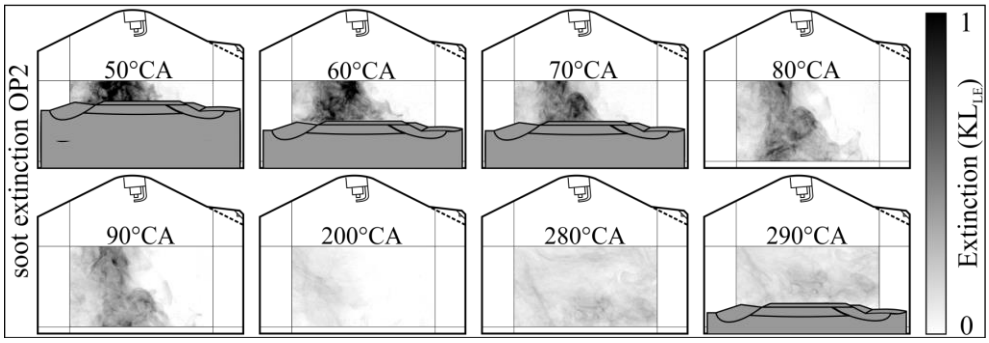

Examples of single shot images of light extinction in the soot particle cloud for OP2 and for E20. Measurements are extracted from (Koegl et al 2019) in which additional data is available. (Annex A, Figure 8)

The extinction images in the figure above show that a local soot formation occurs in the left area of the piston; recalling that the injector is located in the upper right hand of the picture. A high amount of soot can be detected at late points in time during the exhaust stroke (e.g. at 290°CA). The rate of soot oxidation can be estimated from the change of extinction, e.g. when comparing the value at 80°CA and 280°CA. At these two points in time, the piston position and the optically accessible volume of the cylinder is comparable. These points in time and the respective extinction are presented in the next figure for the operating points (OP1 and OP2) and fuel blends studied.

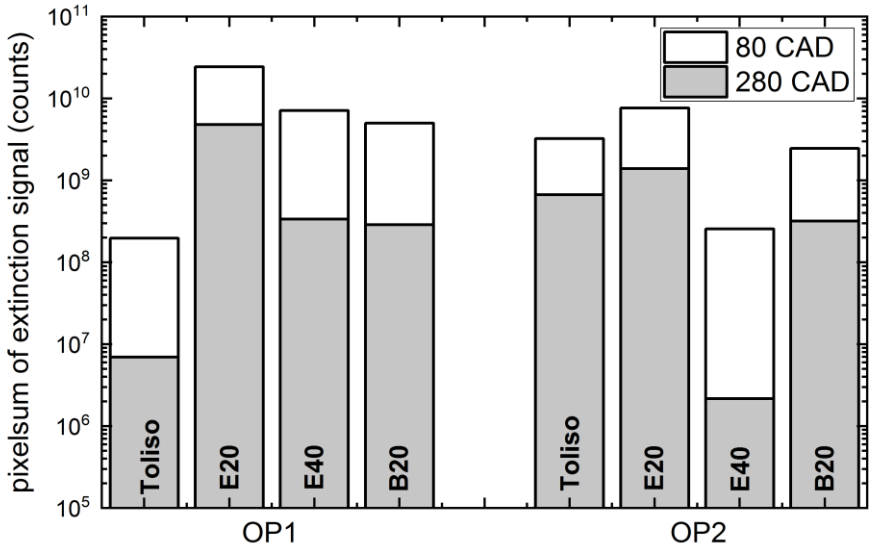

Accumulated averaged extinction signals (note the log-scale) at two points in time for estimation of in-cylinder soot formation and oxidation for Toliso, E20, E40 and B20; some measurements for OP1 are extracted from (Koegl et al 2018) in which additional data is available.

The soot levels indicated by the values at 80 and 280 CAD can be correlated with other measurements in a comprehensive fashion when viewed in conjunction with light extinction measurements conducted during injection (Figure 3, Annex A), and particle concentration measurements in the exhaust (Figures 4&5, Annex A). For example, for OP1 Toliso shows a relatively weak extinction signal and thus soot formation at 80°CA, while at 280 °CA almost all of

the soot is oxidized (i.e. the extinction signal is close to the reference level). E20 shows the largest extinction and thus increased soot formation, which can be explained by the changed evaporation and mixture formation. E40 shows similar sooting behaviour like E20 but at reduced maximum intensities. Still, the formation of soot is larger than for Toliso and higher level of soot is present in the exhaust stroke indicating more incomplete oxidation. The extinction signal of E40 and B20 are comparable in the exhaust stroke (280°CA), i.e. a similar soot concentration is expected for these fuels. Further detailed analysis is available in Annex A and the original references used therein.

Exhaust Gas Measurements in a 4-cylinder metal engine

For the 4-cylinder engine, special operating points with constant load and engine speed were chosen for soot generation and oxidation.

Specifications of the 4-cylinder metal engine. (Annex A, Table 3)

Number of cylinders / valves	4 / 4
Displacement volume (cm^3)	1801
Stroke/bore (mm)	84.1 /82.5
Effective compression ratio	9.6
Injector position	lateral
Injection system	common rail

Operating points of the metal engine (EOI, End Of Injection). (Annex A, Table 4)

Operating point	λ	p_{mi} (bar)	Exhaust mass flow (kg/h)	EOI (bTDC) (°CA)	comment
OP1	0.77	10.0	93.0	310	Filter loading
OP2	1.10	9.0	87.1	270	Oxidation, 500°C at filter outlet
OP3	1.00	9.5	84.7	270	reference
OP4	1.00	9.5	84.7	310	Very early injection
OP5	1.10	12.8	127.6	270	Oxidation, 600°C at filter outlet

Measurements upstream of the soot oxidation filter for different operating points and E20 vs gasoline are compared in Figure 10 (Annex A). With the engine tested in a warm state, E20 showed similar or slightly lower soot volume fractions compared to gasoline.

2.2 Tailpipe emissions from GDI vehicles

The parameters governing the chassis dynamometer tests reported by contributors to Annex 54 have been summarized and compared in Table 1 at the beginning of Section 2. Noteworthy aspects of the experimental procedures and the results are discussed below by country in each of the subsections dedicated to the types of emissions, the effects of fuels, driving type, and after-treatment. This section is organized to include contributions from participants under three considerations for gaseous and particulate tailpipe emissions:

- Effect of alcohol fuel blends on emissions (Section 2.2.1)
  - Gaseous emissions (Section 2.2.1.1)
  - Particulate emissions (Section 2.2.1.2)
- Effect of start-stop operation on emissions (Section 2.2.2)
- Effect of gasoline particulate filters on emissions (Section 2.2.3)

2.2.1 Effect of alcohol fuel blends on emissions

2.2.1.1 Effect of alcohol fuel blends on regulated gaseous emissions

Chile

(Excerpts from Gramsch et al 2017)

Two flex-fueled vehicles using different ethanol blends in gasoline were used to study primary and secondary gas and particle concentrations.

- A 2012 model year flex-fueled Ford Focus 2.0 GDI with a three-way catalyst (TWC), meeting Tier 2, Bin 4 U.S. emission standard.
- A Chevrolet Prisma 1.4 flex-fueled, Econoflex engine, indirect injection, with a three-way catalyst, meeting the PROCONVE L-6 Brazil emission standard.

The U.S. car was tested with pure gasoline (E0) and three standard ethanol blends: 10% (E10), 85% (E85 summer; E85S), and 75% (E75 winter; E75W). The Brazilian car was tested with 22% ethanol (E22) and 100% ethanol (E100).

Methodology

All experiments were performed at the Center for Vehicle Control and Certification (3CV) of Chile's Ministry of Transport and Telecommunications in Maipú, Chile. (Figure 1, Gramsch et al 2017). For each vehicle and fuel blend, primary emissions were measured using the 3CV standard dilute-bag approach described in Regulation No. 83 of the Economic Commission for Europe of the United Nations (EUR-Lex 2015). This procedure is used for regulated gaseous primary emissions of total hydrocarbons (THC), nonmethane hydrocarbons (NMHC), carbon monoxide (CO), nitrogen oxides (NO_x), and carbon dioxide (CO_2) while the vehicle is driven over the New European Driving Cycle (NEDC) consisting of urban (UDC) and extra-urban (EUDC) phases. (Figure 2, Gramsch et al 2017). In addition, a second set of measurements were performed in the smog chamber to be discussed in Section 2.3.1 of this report. Both measurements are independent, and for each vehicle they were performed on different days.

Results

The tabulation (Table 2, Gramsch et al 2017) of data by vehicle, fuel, driving cycle, and

temperature indicate that with few exceptions the cold start driving cycles have higher emissions factors for all pollutants than the hot start cycle and the urban driving emission factors are higher than the extra-urban driving. These are in general agreement with previous measurements by others. There is a tendency to decreased emissions with increasing ethanol content for all regulated emissions but CH_4. Primary emissions of THC, CO, CO_2, and NMHC for both cars decreased as the fraction of ethanol in gasoline increased, which is consistent with previous studies.

Israel

The study using three flex-fueled vehicles (two GDI, one PFI engine) compared regulated and unregulated tailpipe emissions with high percentage alcohol blends (E85, M65) and gasoline (RON95) with the NEDC driving cycle. The vehicles used were:

1) 2014 MY, 2.4 liter, naturally aspirated DI, automatic transmission vehicle, homologated according to US standard, at 77,000 km;
2) 2011 MY, 2.0 liter, Euro 5, turbocharged DI, manual transmission vehicle at 106,000 km.;
3) 2012 MY, 1.6-liter, Euro 5, PFI, manual transmission vehicle at 50,000 km.

The experimental work was conducted at the vehicle emission laboratory (VELA) of the JRC, located in Ispra, Italy. The tests were performed using a standard facility for exhaust emission measurement that complies with the European regulation on type approval.

The results (Figure 1, Annex B) show that using oxygenated fuels could decrease substantially the emissions compared to RON95. While the effect on NOx was relatively small, all the other emissions which include HC, CO, CO_2, and NMHC (with the exception of formaldehyde) decreased. There is no legislation for formaldehyde emissions in the EU but limits are specified in the US and Canada, with the possible carcinogenic effects of formaldehyde being of general concern. Between the two oxygenated fuels M56 caused larger increases in formaldehyde emissions than E85. The pre- and post- particulate results measurements of formaldehyde (Figure 1, Annex B) for all three vehicles show that the TWC was quite effective in reducing these emissions.

2.2.1.2 Effect of alcohol fuel blends on particle emissions

Chile

In this study PM mass was not measured directly using a standard instrument; rather, an effective mass concentration was obtained from the SMPS assuming spherical particles with a density of 1.2 g/cm_3. The main objective of the exercise was to obtain an indication of the contribution of secondary PM to total PM. Further discussion is presented in Section 2.3.1 under Chile.

Germany

The particle matter concentrations in the exhaust of a single cylinder engine (discussed in Section 2.1 above), although not strictly tailpipe emissions, are considered relevant for this section. Particle matter concentrations had been measured under different operating conditions (Annex A, Table 1, also Section 2.1 above) and for different fuels, including alcohol fuel blends.

The following figures summarize particle concentrations measured in the exhaust duct for different operating points and fuels.

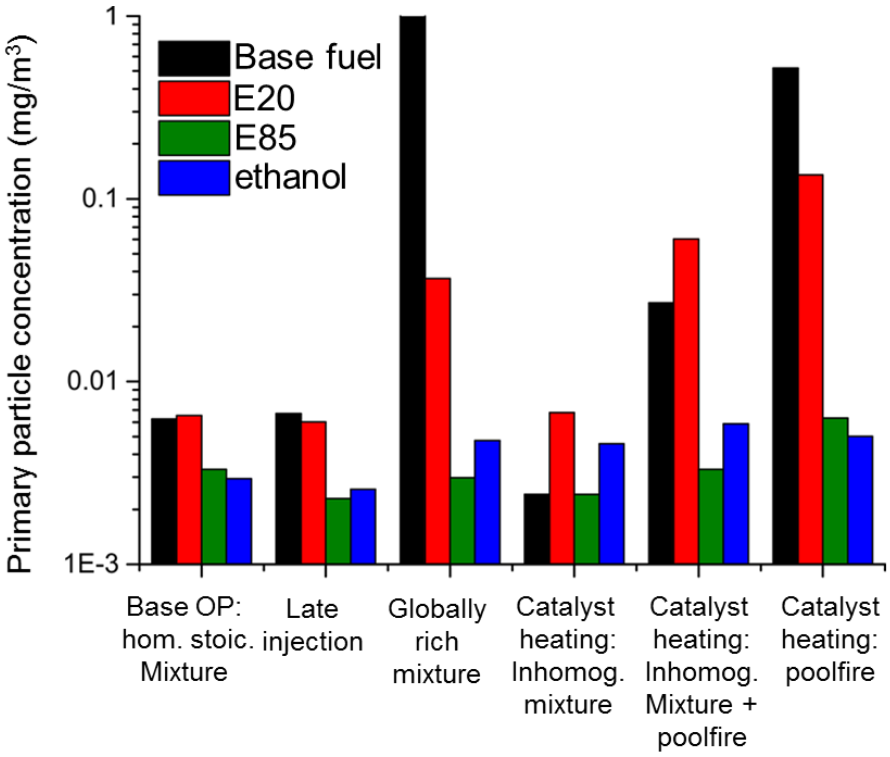

Particulate concentration in exhaust gas for a selection of the investigated operating points and the fuels iso-octane (base fuel), E20, E85 and pure ethanol, measured with the LII exhaust gas sensor. (Annex A, Figure 4)

For all operating points above it can be seen that the particle concentration is largest for E20 and iso-octane. The highest particle concentrations were measured for the operating points "Globally rich mixture" and "Catalyst Heating: Poolfire". The trends of the particle concentrations in the exhaust gas can be correlated with the fuel-dependent results of the soot radiation and light extinction measurements in the cylinder (see Section 2.1, *In-cylinder Soot formation and Oxidation Investigation*).

The next figure (Annex A, Figure 5) shows a comparison of the measured average particle concentration for the previously defined operating points for the pure substances iso-octane, ethanol and n-butanol. For the operating points "base point", "late injection" and "global rich mixture", the exhaust particle emissions of butanol behave similarly to those of ethanol. For butanol, chemical mechanisms (due to the fuel-bound oxygen content) also seem to dominate soot formation for these operating points. Under the "catalyst heating" operating points, a significantly increased particle concentration was detected for butanol. Physical properties of the fuel (e.g. viscosity, enthalpy of vaporization) appear to be the main factor influencing soot formation under these conditions. These properties determine atomization and evaporation and could contribute to wall wetting as well, also examined in Section 2.1.1 *In-cylinder Soot formation and Oxidation Investigation* with relevant butanol mixtures (e.g. B20).

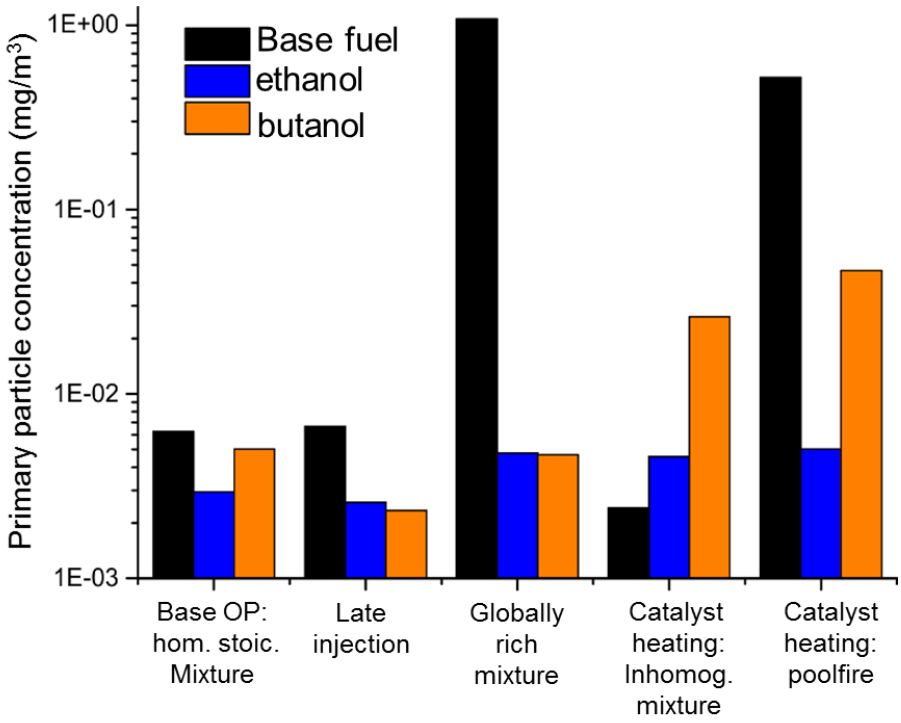

Particle concentration in the exhaust gas for a selection of the investigated operating points and pure substances iso-octane (base fuel), ethanol and n-butanol measured with the LII exhaust gas sensor. (Annex A, Figure 5)

Israel

Comparison of the results between the two direct injection SI engines and the port injection engine suggest that DI SI engines tend to emit more PM/PN compared to PFI engines.

Particulate Mass (PM): Particulate samples were collected according to the modified procedure developed in the framework of the Particle Measurement Program (PMP) and using a Pallflex TX40HI20 filter (one filter per cycle, no secondary filter). The mass was determined by weighing.
Particle Number (PN): Total PN was measured using a system compliant (AVL APC) with the requirement defined in the Particulate Measurement Program (PMP) and now included in UNECE Regulation 83.

PN & PM emissions were decreased substantially with the use of oxygenated fuels, especially for direct injection SI engines (Figure 1, Annex B). It was suggested that given the expected requirements of particulate filters for DI engines, the results of this research suggest that using oxygenated fuels could be an additional measure to the use of GPFs for decreasing PM & PN from DI engines.

2.2.2 Effect of start-stop operation on emissions

United States

Excerpts from (Storey et al 2019)

The contribution from United States focused exclusively on the effect of start-stop operation which has become common in light duty vehicles. The motivation is essentially to improve fuel economy, particularly in city driving: “During start-stop operation, the engine shuts off when the

vehicle is stationary for more than a few seconds. When the brake is released by the driver, the engine restarts. Depending on traffic conditions, start-stop operation can result in fuel savings from a few percent to close to 10%." GDI engines also share this fuel economy motivation but are burdened with higher PM emissions, particularly during start-up transients. It was therefore of interest to study the emissions from a start-stop operation enabled GDI vehicle to determine the effect of this feature.

Methodology

A 2014 Chevrolet Malibu Eco equipped with a 2.5L GDI engine and start-stop operation was selected. The start-stop operation is active once the engine warms up and can be disabled by opening the hood. The regulatory test FTP-75 has periods of idle in the driving cycle that can stop the engine when start-stop is enabled and tests were carried out using both cold and hot started FTP-75 phases with three different fuels: gasoline, an ethanol blend (E21), and an isobutanol blend (iBu12). Multiple repeats were run for each mode (hot or cold start) and fuel combination, 3 for cold starts and 27 for hot starts, anticipating the inherent variability of the processes which can lead to higher PM emissions in GDI engines. In addition to gravimetric filter based particulate mass measurements, real-time particulate soot mass was obtained from a photoacoustic-based Micro Soot Sensor™ (MSS, AVL Model 483) and real-time particle size and number were obtained with an Engine Exhaust Particle Sizer (EEPS™). Gaseous emissions were measured with standard procedures/equipment.

Results

PM mass emissions, gravimetrically from filter samples

The effects of start-stop operation and differences between E0 (i.e. 87 AKI gasoline) and E21 on composite PM mass emissions over the FTP driving cycle are relatively small but have some interesting aspects (Storey et al 2019, Figure 4). Both E0 and E21 had composite PM mass emissions less than the 3 mg/mi US Tier 3 limit, with iBu12 noticeably higher. E21 emissions were lower than E0 for start-stop operation although they were about the same for no start-stop. The emissions for E0 were higher for start-stop operation while the effect is actually reverse for E21 with start-stop operation giving lower emissions than no start-stop operation. When emissions separately over the cold and hot started phases of the FTP are examined (Storey et al 2019, Figure 5) it is clear that the cold FTP mass emissions are by far the most significant contribution to the composite emissions.

Transient soot and PN measurements

The high frequency (1 Hz) measurements of particle number with the EEPS and soot mass with the MSS were used with the simultaneous flowrate data and integrated over the duration of the FTP phases to arrive at #/mi and mg/mi results for cold and hot started FTP phases (Storey et al 2019, Figures 6 & 7). Given the variability of data over multiple cycles, the average values of #/mi data suggest that the mode (start-stop and no start-stop) makes little difference for E0 and E21 PN emissions for both the cold and hot started FTP phase. Similarly, there is no clear influence of start-stop on the soot emissions for any of the fuels during the cold started phases although there does appear to be soot emissions impact from the mode during the hot started phases, especially for the iBu12 fuel which saw a significant soot mass increase during start-stop operation.

The available transient data was also examined along with the speed traces of the FTP phases, indicating the strong correlation between elevated emissions of both particle number and soot mass measurements with acceleration events, although the cold vs. hot start phases had a much stronger effect on the level of emissions (Storey et al 2019, Figures 8-11).

Conclusion

"A major conclusion of this study was that while some difference could be seen in particulate emissions, the difference in PM mass emissions was not very large between start-stop and no start-stop operation for this vehicle, suggesting that the additional starts are unlikely to significantly increase the PM emissions. If this vehicle is representative of the market, this finding is important as GDI engines penetrate the light-duty market and more manufacturers adopt start-stop for fuel economy."

2.2.3 Effect of gasoline particulate filters (GPFs) on emissions

Canada

Excerpts from (Araji & Stokes, 2019)

Methodology

The goal of the study was to investigate the emission impacts of replacing the OEM three-way catalyst on light duty trucks using various, commercially available, gasoline particulate filter (GPF) configurations. Three light duty trucks were tested: a Port Fuel Injection (PFI_1) and two Gasoline Direct Injection vehicles (GDI_1 and GDI_2). The testing of these vehicles was conducted on a chassis dynamometer in a controlled test cell environment at two temperatures (25 °C and -7 °C) using the FTP-75 and US06 test procedures. All three vehicles were tested in stock OEM configuration followed by testing PFI_1 and GDI_1 with a non-catalyzed GPF and GDI_2 with a catalyzed GPF. GDI_2 was also tested on-road using a portable emissions measurement system with and without the use of the catalyzed GPF.

Both non-catalyzed (uncoated) and catalyzed (coated) GPF systems were wall flow filters made of Cordierite ceramic with an approximate wall thickness of 8 mil. In both configurations the GPF replaced the catalytic converter in the close-coupled position (Araji & Stokes, 2019, Figure 1). All GPFs used were in a clean state at the start of testing, with no mileage accumulation or pre-conditioning.

Results

Total Particulate Mass and NOx Emissions

Filtration efficiencies (based on percentage of mass collected) tabulated for the two driving cycles and operating temperatures ranged between 53% and 89% over the FTP-75 cycle, and between 46% and 72% over the US06 cycle (Table 3, Figures 2-4, Araji & Stokes, 2019). The effect of operating temperature on the efficiencies for the vehicles with catalyzed and non-catalyzed GPFs were not consistent for the two cycles showing increase with temperature over the USO6 for the catalyzed GPF but a decrease for the non-catalyzed GPF. The lower efficiency of the catalyzed GPF (53% compared to 89% for the non-catalyzed GPF, both for FTP-75 at 25 C) was attributed to the effect of the porosity of the fresh coating in the catalyzed GPF.

Black Carbon Emissions

The laser-induced incandescence measurement (Artium LII 300) of black carbon mass enables the monitoring of BC accumulation over the test cycle (Figures 5-10, Araji & Stokes, 2019). For the FTP-75 cycle most of the BC mass accumulated in the first 505 seconds which represents phase one of the test cycle and captures the cold start emissions. For US06 the increase was more gradual throughout the test cycle with spikes in BC mass which coincided with

accelerations as shown on the speed trace. Filtration efficiency based on BC mass (Table 4, Araji & Stokes, 2019) was observed to be lower in the catalyzed GPF configuration for both the FTP-75 and US06 test cycles and at both testing temperatures. This was also attributed to the fresh-coated filter effect mentioned under PM mass.

Particle Number (PN) Emissions and Particle Size Distribution

Filtration efficiencies (based on the reduction in #/mile results) tabulated for the two driving cycles and operating temperatures were in the 52-86% range (Tables 5 & 6, Araji & Stokes, 2019) with the exception of the GDI vehicle with the non-catalyzed GPF showing an increase in emissions with the GPF, resulting in a nominal -38% reduction efficiency for the FTP-75 at -7 C. Particle size distribution measurements provide some insight for this result with a clear shift to lower particle sizes for this particular combination of driving cycle and operating temperature (Figure 13, Araji & Stokes, 2019). Whereas the other 3 FTP-75 runs for this vehicle (OEM and GPF at 25 C, OEM at -7 C) showed broad size distributions peaking around 70 nm, the size distribution for the GPF run at -7 shows a sharper peak around 10 nm. "Although further investigation into this phenomenon would be necessary to draw a definitive cause, a potential reason for a heightened level of particles at this size would be smaller particles slipping through the fresh filter after cold start accelerations or the result of a partial regeneration of the filter."

Other notable trends in particle size distributions are that the PFI vehicle (with a non-catalyzed GPF) had a bimodal distribution with peaks at 8 nm and 60 nm for all tests with and without a GPF and for both test cycles and test temperatures (Figures 11&12, Araji & Stokes, 2019), while the GDI vehicle with the catalyzed GPF had unimodal distributions generally (Figure 15, Araji & Stokes, 2019) similar to the 3 cases mentioned above (Figure 13, Araji & Stokes, 2019) for the non-catalyzed GPF. Other distributions in tests (Figures 14, 16) point to the complexities that arise in tailpipe measurements that are not always amenable to direct interpretation.

Gaseous Emissions

The PFI vehicle (non-catalyzed GPF) showed some increase in CO and NOx emissions relative to the OEM configuration with both driving cycles at 25 C (only operating temperature for the PFI vehicle). An increase in THC was also noticed for the US06 cycle. (Figure 17, Araji & Stokes, 2019) . Since the GPF had replaced the reduction catalyst in the close-coupled position of the OEM configuration (Figure 1, Araji & Stokes, 2019) , the increase in NOx was expected. The replacement of the reduction catalyst could also explain the increases in CO and THC due to the loss of the oxidation action from the smaller amounts of Palladium in the replaced reduction catalyst.

The GDI vehicle with the non-catalyst GPF also showed increases in NOx emissions relative to the OEM configuration with both driving cycles and operation temperatures. There was an increase in THC during the FTP-75 tests at 25 °C and the US06 tests at 25 °C and -7 °C. However there was no significant difference in CO and CO_2.

The GDI vehicle with the catalyst GPF showed a decrease in NOx emissions (in contrast to the previous two cases above) with the US06 driving cycle at both operating temperatures (Figure 19, Araji & Stokes, 2019). There was no significant difference in CO, CO_2 and THC. To eliminate any back pressure challenges the catalyzed GPF had been designed physically bigger than the OEM reduction catalyst, thus increasing the residence time and possibly accounting for the increased treatment for NOx.

Switzerland

Excerpts from (AFHB 2016, Empa 2017)

Methodology

Four different prototype particle filters supplied by two industrial partners were used in the study. Two GPFs were non-coated, two were coated with unspecified catalytic material. The four filters named GPF-1, -2, -3 and -4, were installed at the tailpipe of the reference vehicle (Volvo V60, 1.6 L, Euro-5) and tested under similar conditions in the cold and hot started WLTC and the SSC. The tests enabled the study of the Impact of GPFs on particle size distribution, the efficiencies of GPFs in reducing particle number emissions, and the impact of GPFs on genotoxic PAH emissions.

Results

Impact of GPFs on particle size distribution

Particle size distributions were determined simultaneously using SMPS and nano-SMPS, data correlating well in the overlapping size range thus enabling the observation of sub-23 nm particles with the nano-SMPS.

A bimodal particle size distribution with nucleation mode particles at 20 nm and accumulation mode particles at 80 nm with indication of an increase towards 10 nm was observed without GPF for the reference vehicle under steady state driving at 95 km/h. With GPF, particle emissions were lowered by 2-3 orders of magnitude, resulting in particle number concentrations in the range of 2x10e2 to 6x10e5 particles/ccm in dilute exhaust. PN filtration efficiencies were greater than 99% throughout the size range even for the very fine particles less than 30 nm without the increase towards 10 nm observed in the absence of GPF.

Efficiencies of GPFs and particle number emissions

Particle number emissions (particles/km) of the reference GDI vehicle (Volvo V60, 1.6 L, Euro-5) were measured in the cold and hot started WLTC and the SSC with each the GPFs. Comparisons were made with the emissions of the reference vehicle without GPF as well as the benchmark diesel vehicle (Peugeot 4008, 1.6 L, Euro-5) with DPF . GPF-1 showed the highest efficiencies reducing PN emissions by 1 to 2 orders of magnitude at transient driving in the cold and hot WLTC, and by 3 orders of magnitude under steady vehicle operation (SSC). PN emissions after this filter were still about a factor 10 higher than those of the diesel vehicle, but were more than one order of magnitude lower than those after GPF-2, -3 and -4.

On average, the four prototype GPFs achieved PN reductions of 77%, 87% and 95% in the cWLTC, hWLTC and the SSC respectively, thus enabling the retrofitted reference vehicle to have emissions below the actual PN limit of 6 x 10e11 particles/km. It was also noted that this is unlikely to be representative of the maximum efficiency that can be achieved with well integrated filter technology, as shown by the bench mark diesel vehicle with a well-integrated and regulated catalytic DPF.

Impact of GPFs on genotoxic PAH emissions

(Discussed under Switzerland in Section 2.3.2*)*

2.3 Secondary organic aerosol formation and genotoxic potential

The human health effects of atmospheric particulate matter are due to both the primary emissions of particulate matter from vehicle tailpipes and the secondary particulate matter that forms in the atmosphere from gaseous emissions in vehicle exhaust. It is therefore of interest to be able to quantify both of these sources associated with vehicle emissions. Although primary emissions of PM are subject to regulation, the secondary aerosol formation potential is challenging to measure. Furthermore, the secondary aerosol formation from vehicle exhaust depends on the characteristics of the air shed into which the vehicle exhaust is emitted and is therefore challenging to quantify. Nevertheless, there is accumulated research addressing the related questions, including the work reviewed below in Section 2.3.1.

Genotoxicity describes the property of chemical agents to damage the genetic information within cells, causing mutations which may lead to cancer. Polycyclic aromatic hydrocarbon compounds are semi-volatile compounds which are partial products of combustion processes that can be found in both the gaseous and particulate phases of tailpipe emissions from gasoline and diesel vehicles. The US EPA lists 16 PAH compounds in its priority substances list (U.S. EPA 2014). Eight PAH compounds have been classified as carcinogens by the World Health Organization (Munoz et al 2016). Systems of equivalent toxicity in terms of the toxicity of one member of the PAH family have been adopted in assessing health risk associated with mixtures of polycyclic aromatic hydrocarbons (Petry et al 1996). Among the submissions for Annex 54, the report from Switzerland (Empa, 2017) presents experimental work on genotoxic potential and PAH emissions and is described in a dedicated section further below.

2.3.1 Secondary Organic Aerosol formation potential

Chile

Excerpts from (Gramsch et al 2018)

The SOA formation potential study was performed using a Teflon-lined smog chamber of 14 cubic meters designed and developed at the Harvard T.H. Chan School of Public Health (HSPH) in Boston, Massachusetts, USA (Figure 1, Gramsch et al 2018). The basic methodology involved filling the chamber with the diluted exhaust from the vehicle/fuel combination being tested and monitoring the concentrations of gaseous species and aerosol over several hours. The experiments were performed in the chamber, and measurements were done with a different set of instruments than what was used for emission measurements detailed in Section 2.2.3.1.

Methodology

Ozone formation inside the chamber during irradiation was measured by means of an ozone monitor (model 202; 2BTEC). A portable CPC (model 3007; TSI) was used to measure particle count concentration. An NO/NO_y (with $NO_y = NO + NO_2$ + other nitrogen oxides) monitor was used to monitor continuous concentrations of $NO/NO_2/NO_x$ before and during irradiation. Chamber temperature and relative humidity (RH) were monitored by means of a temperature/relative humidity sensor. To monitor the size distribution of particles between 15 and 700 nm, a scanning mobility particle sizer (SMPS) with an electrostatic classifier (TSI model 3934) was used. A differential mobility analyzer (DMA; model 3081; TSI) based on Electrostatic Classifier 3080, running with Aerosol Instrument Manager software (version 9, TSI) and coupled

with a water-based condensation particle counter (CPC; model 3785; TSI), was used to obtain continuous particle number information.

PM mass was not measured directly using a standard instrument; rather, an effective mass concentration was obtained from the SMPS assuming spherical particles with a density of 1.2 g/cm^3. To obtain the ratio of secondary to primary PM concentration, the mass was estimated using the SMPS before the lights were turned on and when the mass concentration reached the maximum. The ratio was calculated after subtracting the primary mass concentration. The SMPS used in this study measured particles larger than 14 nm and had low efficiency for particles lower than ~25 nm.

Results

Secondary gas formation

The general trend in gaseous species (Figure 6, Gramsch et al 2018) in the chamber is for NO to start from the maximum value observed just before the UV lamps are turned on and decrease with time as NO_2 is generated. The instrument measures NO_y and NO and reports as NO_2 the difference of [NO_y – NO]. Both NO_2 and O_3 go through a peak as the photochemical reactions proceed.

There is a notable difference between the results with the two vehicles, the Chevrolet Prisma, giving much higher NO concentration at the beginning of the experiment than the Ford Focus, attributed to the difference in car technology. Ultimately, as the photochemical reactions progress Figure 6 shows that when NO_2 concentration reaches the maximum, the amount of NO in the Chevrolet Prisma is about 150 ppb, whereas in the Ford Focus, the amount of NO is about 35 ppb.

The maximum concentration of NO and [NO_y – NO] seems to be dependent on the amount of ethanol on the gasoline and the type of engine (Figure 7, Gramsch et al 2018). In the Ford Focus, there is a tendency to generate more NO with higher ethanol content. For the Chevrolet Prisma, lower formation of NO and [NO_y – NO] is observed for E100. Another difference between blends and car types is the time that it takes to reach the maximum concentration for [NO_y – NO] and O_3 (Table 4, Gramsch et al 2018). The shortest time to reach the maximum formation of [NO_y – NO] occurs for the Ford Focus with the E0 blend (45 min). As the fraction of ethanol increases, the time increases, and reaching 110 min for the E85S blend. Similar trend occurs for O_3 in the Ford Focus. For the Chevrolet Prisma, the time to reach the [NO_y – NO] maximum is longer for E100 than for the E22 blend.

Secondary particle formation

To obtain the ratio of secondary to primary PM concentration, the mass was estimated using the SMPS before the lights were turned on and when the mass concentration reached the maximum. The ratio was calculated after subtracting the primary mass concentration.

Although some factors are acknowledged that introduce uncertainty into the primary and secondary PM calculations, and the ratios obtained in this way, the results indicate that for both cars there is a decrease in primary mass concentration when the ethanol content in fuel increases (Figure 8, Gramsch et al 2018). Secondary to primary PM ratios are also shown in Figure 8 and increased with increased ethanol content for Ford Focus (the “American car”), but decreased in the Chevrolet Prizma (the “Brazilian car”).

For both vehicles, the time required to form secondary PM is longer for higher ethanol blends, which may be related to lower emission of aromatic compounds. These results indicate that using higher ethanol blends may have a positive impact on air quality.

Switzerland

Excerpts from (Empa 2017)

Three independent approaches are reported in Switzerland's contribution addressing issues related to SOA formation potential of vehicle exhaust:

- mobile smog chamber (SC)
- potential aerosol mass (PAM) oxidation flow reactor (OFR)
- micro smog chamber (MSC)

The first two studies were conducted at the Paul Scherrer Institute (PSI), while the third study was conducted at the University of Applied Sciences Northwestern Switzerland (UASNW)

Experimental set-up at the Paul Scherrer Institute

The complete details of the mobile smog chamber and the potential aerosol mass oxidation flow reactor studies are available in (Pieber et al 2018). The following picture (Figure 24, Empa 2017) below provides a summary overview.

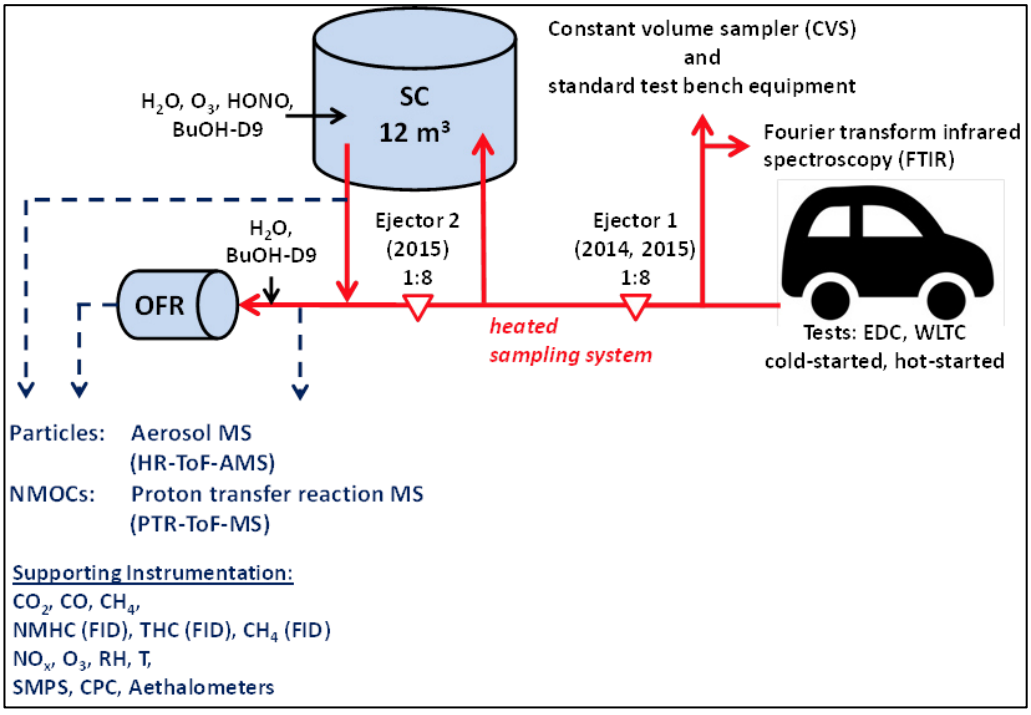

The photochemical activity of vehicle exhaust was studied by first extracting diluted exhaust samples from the constant volume system (CVS) and directing it to either the smog chamber (SC) or the oxidation flow reactor (OFR) (Pieber et al 2018). The 12 cubic meter SC could be used either for storing (UV lamps off) a batch sample of emissions over different phases of a driving cycle for later study in the OFR, or be photochemically aged (UV lamps on) in the smog chamber

itself over a 2 hour period. The OFR with a residence time of 90-100 seconds enabled the real time characterization of emissions extracted directly from the CVS during different phases of the driving cycles, as well as being used to study the photochemical aging of stored batch samples from the smog chamber. The associated chemical instrumentation enabled the characterization of either fresh (directly from CVS) or aged (photochemically in the SC or OFR) samples.

Chemical instrumentation included a high resolution proton transfer reaction time-of-flight mass spectrometer (PTR-ToF-MS) to study the chemical composition of the gaseous organic compounds in fresh and aged emissions; a high resolution time-of-flight aerosol mass spectrometer (HR-ToF-AMS) to provide quantitative, size-resolved mass spectra of the non-refractory sub-micron particle composition; as well instrumentation for CO_2, CO, CH_4, NMHC, THC, NO_x, O_3, RH, SMPS, CPC, and Aetholometers.

The experiments were conducted over two years, using 4 different GDI vehicles and the WLTC and EDC driving cycles as summarized in the table below (Table 2, Empa 2017).
Experiments were conducted in three configurations: 1) time-resolved measurements of primary emissions and time-resolved aging in the oxidation flow reactor, 2) OFR photochemical aging from SC batch samples, 3) SC photochemical aging of SC batch sample

Table 2. Vehicles and tests (*n* number of tests conducted; EDC tests were only conducted with GDI-1 and GDI-1 w/GPF).

Vehicle Code	Vehicle Type	Expt. Set	cold-started WLTC	hot-started WLTC	cold-started EDC	hot-started EDC
GDI-1	Opel Insignia; Euro 5, standard configuration	2014 (I)	*n*=4	*n*=4	*n*=1	*n*=1
GDI-1 w/GPF	Opel Insignia; Euro 5, with retrofitted GPF (underfloor)	2014 (I)	*n*=4	*n*=4	*n*=3	*n*=3
GDI-2	Opel Zafira Tourer, Euro 5	2015 (II)	*n*=4	*n*=4	--	--
GDI-3	VW Golf Plus, Euro 4	2015 (II)	*n*=4	*n*=4	--	--
GDI-4 (2014)	Volvo V60, Euro 5, standard configuration	2014 (I)	*n*=4	*n*=4	--	--
GDI-4 (2015)	Volvo V60, Euro 5, standard configuration	2015 (II)	*n*=3	*n*=1	--	--
GDI-4 w/GPF	Volvo V60, Euro 5, with retrofitted GPF (underfloor)	2015 (II)	*n*=4	*n*=2	--	--
GDI-4 w/catGPF	Volvo V60, Euro 5, with retrofitted catGPF (underfloor)	2015 (II)	*n*=4	*n*=2	--	--

Results

Pollutants as function of vehicle technology and driving cycle

Investigation of THC, NMHC and gravimetric PM of time-resolved emissions for cold- and hot-started WLTC and EDC tests using the GDI1-3 vehicle demonstrated significant THC and NMHC emissions during cold-engine tests, with emission factors reduced by a factor of 90 during hot-started cycles. Emission factors from cold-started WLTC for this vehicle were dominated by phase 1 which exceeded all other phases of the WLTC by 2 to 4 orders of magnitude. Vehicle GDI4

had lower total emissions during cold-started cycles compared to other vehicles and a smaller difference between cold- and hot-started cycles (only 8 times higher, rather than 90 times as for GDI1-3). Lower cold start emissions of GDI4 compared to other vehicles may be explained by differences in the catalytic after-treatment system, the location of the catalyst as well as reduced cold start enrichment. In terms of NMHC/THC emission factors GDI4 can be considered in line with Euro 6 vehicles, for which regulation also focuses on the reduction of the cold-start HC emissions.

Effects of gasoline particle filters (GPF) on SOA

While the retrofitted GPFs efficiently remove the non-volatile black carbon and thus significantly reduce total primary PM, the effect on primary organic aerosol (POA) is more complex. POA has a wide range of volatilities and may thus encounter a particle filter in either vapor or particle phase. Thus GPFs can only efficiently remove the low volatility POA fraction, while more volatile POA passes through the filter as vapor and will condense when the exhaust is cooled in the ambient air. Within experimental uncertainty, retrofitted GPFs (including catGPF behind the standard TWC) did not affect the POA fraction.

Conclusions on SOA formation

GPF application efficiently removes elemental black carbon particles, which is the dominant component of primary PM, but has small effects on the minor POA fraction. The volatile POA fraction passes through the filter in the vapor phase and later condenses when the exhaust is emitted and cooled; hence POA emission factors are not significantly reduced by GPFs and SOA formation was not affected by the tested GPFs, neither by non-coated nor by catalyst coated GPFs. This means that retrofitting GDI vehicles with GPFs will result in an important reduction of the total primary PM emitted (removal of refractory material), but will not, or only to a small extent, reduce hydrocarbon emissions including benzene and alkylbenzenes and will not directly lead to a reduction of the SOA formation. Future work on so-called 4-way catalysts, i.e. a TWC catalyst directly applied onto a GPF and installed at the location of the current TWC for simultaneous filtration of particulates and catalytic conversion of hydrocarbons should be conducted to understand, whether reductions of SOA precursors, SOA production, and semi-volatile primary PM can also be achieved.

Accelerated SOA formation in the UASNWS flow reactor

An even faster flow reactor allowing the determination of the SOA formation potential of a vehicle exhaust per second during transient vehicle operation was developed by the UASNWS (Figure 31, Empa 2017)

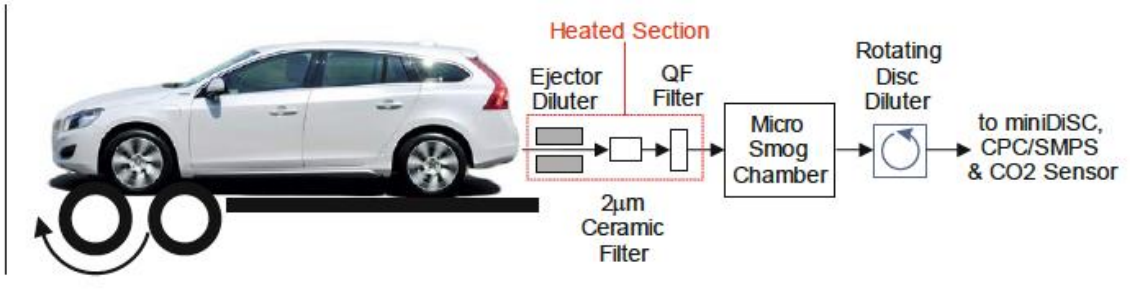

Figure 31: Schematic representation of the experimental setup using the MSC.

GDI exhaust samples are extracted during the driving cycle or during steady state conditions (constant speed or idle). Exhausts are filtered to remove primary particle and only the gas-phase fraction (dilution ~1:10 at 150 C) is oxidized inside the micro smog chamber. This produces nucleation particles composed purely of secondary aerosol. On a second dilution stage, the concentration is reduced to levels compatible with aerosol measurement devices. The continuous-flow reactor-tube was applied to study the formation of secondary aerosols by taking the gas-phase fraction of exhausts and oxidize it with ozone (up to 60 ppm) at residence times of about 10 seconds. Integration of time-resolved SOA data from CVS exhausts allows deducing mean SOA emission factors (mg/km) of different GDI vehicles in different cycle phases.

Results

Compared to the results from the PAM reactor and the smog chamber at the Paul Scherrer Institute in the previous section, the micro-smog chamber produced lower levels of secondary aerosols. This is attributed to the differences in the humidity content of the sampled exhaust by the two methodologies. The PAM reactor humidifies the sample close to 90% RH before exposing it to UV light which boosts the OH reactions that lead to formation of SOA. In contrast, the micro-smog chamber relies on the humidity already present in the sample, which in previous applications, like e.g. biomass combustion emission, is high enough for this processes to take place. But in the case of the GDI vehicles exhaust, the relative humidity was already low in the raw gas. Thus, aging in the micro-smog chamber was dominated by ozonolysis, whereas aging on the PAM reactor and the smog-chamber includes both ozonolysis and OH reactions. With the benefit of the experience with the completed work it is expected that the micro-smog chamber as the smallest and fastest of the three reactors could be easily adapted as a conditioning system for portable emission measurement devices.

2.3.2 Genotoxic potential of non-filtered GDI exhausts

Switzerland

Excerpts from (AFHB 2016, Empa 2017)

Methodology

The experimental details of the chassis dynamometer tests with five GDI and two diesel light duty vehicles have been summarized above in previous sections. For the PAH measurements dilute exhausts were sampled from the CVS tunnel for all vehicle configurations. Concentrations of individual PAHs in non-diluted exhausts of five Euro-3, -4 and Euro-5 GDI vehicles in the hot-started WLTC were compared with PAH concentrations in the exhaust of the Euro-5 diesel vehicle with DPF. The emissions of 4- to 5-ring PAH compounds from most GDI vehicles exceeded those of the benchmark diesel vehicle, whereas those of the less volatile 6- and 7-ring PAHs were comparable to the emissions of the diesel vehicle. Emissions of individual PAHs showed significant variation (one to two orders of magnitude) among different GDI-vehicles.

Using the toxicity equivalents approach for the eight PAH compounds, the genotoxic potential of the emissions from GDI vehicles were compared with the benchmark diesel vehicle equipped with a particle filter in the cold-started WLTC. In all cases the GDI vehicles released more PAHs than the benchmark diesel vehicle. It was noted that the co-release of nanoparticles in large numbers in GDI vehicles presents an effective means of transporting these PAHs into human lungs by first adsorbing onto the nanoparticles.

Results

Impact of ethanol fuel blends on genotoxic emissions

The effect of ethanol blending on genotoxic emissions for a GDI vehicle was studied with the Euro-5 GDI vehicle (Volvo, V60, 1.6 L) operated with gasoline (E0) and two gasoline/ethanol blends (E10, E85) in cold- and hot-started WLTC and under state state conditions (SSC).

PAH emissions were highest in the cold- and hot-started WLTC with gasoline (E0) and were often minimal under steady state operation. This trend was independent of the fuel and was also observed for E10 and E85. Individual PAH emissions in the SSC were sometimes very low, at levels of the dilution air.

Emissions decreased with increasing ethanol levels when comparing E0, E10 and E85 data, both in the cold- and hot-started WLTCs. Higher PAH reduction efficiencies were observed with higher ethanol content and larger ring number, e.g. from70% for 2-ring PAHs to about 95% for 6-ring PAHs when comparing E10 with E0 data, from 85% for 2-ring to 95% for 6-ring PAHs when comparing E85 with E0, all for the hot WLTC. More scatter was noticed in the cold start data without disturbing the general trend.

Looking at the combined genotoxic potential of the eight carcinogenic PAH compounds ethanol blending gave substantial reductions, most pronounced in the hot WLTC with reductions of 77% and 84% for E10 and E85 respectively. Effects were less pronounced in the cold WLTC but pointed in the same direction.

Ethanol blending thus had a strongly favorable effect on the PAH emissions and the genotoxic potential of these emissions for this vehicle, along with favorable effects on emissions of particles, CO, THCs and CO_2. It was noted that additional GDI vehicles have to be studied before generalizations can be made. A testing campaign is underway with two additional GDI vehicles operated with E0 and E10, and with an n-butanol/gasoline blend, containing 15% n-butanol (B15). Results are expected to be available for publishing later.

Impact of gasoline particulate filters on genotoxic emissions

Gasoline particle filters GPF-1, -2 and -3 lowered emissions of genotoxic PAHs by about 45-70% in the cold and by 71- 83% in the hot WLTC, respectively. GPF-4, which was not coated, not only had moderate efficiency with respect to particle number emissions, its impact on genotoxic emissions were only 10% in the cWLTC. In the hot WLTC, even 2- times more genotoxic PAHs were released after the filter than from the vehicle.

It was concluded that GPFs have a large potential to reduce both nanoparticle emissions and genotoxic PAHs but fully integrated catalytic GPFs, operated at higher temperatures, allowing a combustion of accumulated soot and adsorbates, will be needed to lower the genotoxic potential of GDI vehicle exhausts to levels already achieved for diesel vehicles. It was recommended that such GPFs filters should be implemented quickly in GDI vehicles on a global scale.

Metal Emissions

Metal emissions associated with the GDI particles were also addressed by two approaches. In the first approach, diluted CVS exhausts during transient vehicle operation in the WLTC were collected with impingers. Elemental analyses of the impinging solutions indicated that metal

concentrations in dilute vehicle exhausts were as low as those of the dilution air.

In the second approach, non-diluted exhausts were collected with an electrical low pressure impactor (ELPI) which allows size-classified particle sampling in the size range of 29nm to 10µm (aerodynamic diameter). Metal contents of GDI soot, collected on different ELPI filter stages, were very low, mostly at levels of the blank filters. With metal contents at background levels, no obvious differences could be observed for filtered and non-filtered samples or for samples obtained from combustion of gasoline or ethanol/gasoline blends.

3. Key findings

Results obtained during the studies reviewed in this report contribute to a body of literature that has seen rapid accumulation in the past decade. Below, the current scene concerning GDI vehicles is first summarized with the help of three recent publications (Karavalakis et al 2018, Raza et al 2018, Yang et al 2018) before discussing the key results from the studies that are the subject of the Annex 54 report.

3.1 Observations from recent literature

Yang et al (2018), assess the gaseous, particulate, and genotoxic pollutants from two current technology gasoline direct injection vehicles when tested in their original configuration and with a catalyzed gasoline particulate filter(GPF). In addition to the results and analysis from their study they also present a succinct "state of the art" in their Introduction section highlighting:

- The rapid market penetration of GDI vehicles leading governments to impose stricter standards to control PM emissions.
- The challenge for automotive manufacturers in meeting PM reductions in GDI platforms and the combination of measures being considered, including alternative fuel formulations, fuel injection strategies, and the use of gasoline particulate filters (GPFs).
- Studies reporting that the use of oxygenated fuels (i.e., ethanol) have generally beneficial impacts on PM emissions.
- Studies showing that centrally mounted injection systems have lower particulate mass and particle number emissions than wall-guided injection systems because the injector is located close to the spark plug, leading to better fuel evaporation and less wall wetting effects.
- The need for the use of GPFs in GDI vehicles to meet future tightened regulations, particularly in the EU.
- The importance of better understanding the toxicity of the particles being formed in GDI combustion, citing the scarcity of literature about the toxic properties of PM emissions from GDI vehicles, such as those of polycyclic aromatic hydrocarbons (PAHs) and their oxygenated (oxy-PAHs) and nitrated derivatives (nitro-PAHs).

Raza et al (2018) present a comprehensive literature review on (PN) emissions from GDI Engines, describing the characteristics of PM number emitted from GDI engines including chemical composition, size distributions, and PM formation. The effect of combustion parameters influencing PM number emissions such as injection timing, ignition timing, air-fuel ratio, and injection pressure are discussed. The impact of fuel composition, including the effect of certain common oxygenate components (ethanol, methanol, and isobutanol), on PM emissions and PM reduction technologies for GDI engines are also reviewed.

Karavalakis et al (2018) conducted a comprehensive literature review targeting both PFI and GDI engines, and applied statistical analysis related to the effects of gasoline properties, such as aromatics, octane indices, and fuel volatility, on PM (mass and number) emissions from these vehicles/engines. In total, 1841 test results (predominantly in the 2006 to 2010 model year range)for PFI vehicles and 1325 test results (model year 2011-2015) for GDI vehicles were identified for the database.

It is noteworthy that for the purpose of the literature review, the fuels used in individual studies with spark-ignition engines were all treated as gasoline fuels. Although a number of studies used ethanol blends (ranging primarily from 0% to 20% by volume, with the exception of some which included fuels with an ethanol content as high as 83% by volume), butanol blends, and other alcohol fuel formulations, further separation of these fuel types was considered beyond the scope of the analysis.

Statistical analyses were performed separately for PFI vehicles and GDI vehicles. For each of these two vehicle categories, correlations were made for PM mass, total particle number (PN), and solid particle number (SPN) emissions and selected fuel properties that included distillation characteristics (i.e., T10, T50, T70, T90, and EP)[4], aromatics content, Research Octane Number (RON), Motor Octane Number (MON), and Anti-Knock Index (AKI). Additional parameters were also investigated, which included engine type, injection system, engine breathing strategy, number of engine cylinders, and driving cycle. The driving cycles were categorized as FTP, LA92, US06, NEDC, and 'others'.

For GDI vehicles, aromatics and distillation temperatures had the strongest positive correlations with PM mass and total PN emissions, with increasing levels leading to higher emissions. For distillation temperatures, EP was statistically significant for both PM mass and total PN, while T70 and T90 showed a consistent positive correlation only for total PN. The positive correlation for aromatics and distillation temperatures with PM mass/PN emissions is consistent with trends seen for the PMI[5] index, which is a function of higher double bond equivalent and boiling point species. Other properties, such as octane indices AKI, RON, and MON, and T10, generally showed more negative correlations with PM and PN for GDI vehicles. AKI, RON, and MON, showed negative correlations for PM mass, while MON showed a negative correlation for total PN emissions.

A key finding of this study was that for many fuel properties there were statistically significant interactions between the fuel property and either engine type, number of cylinders, and/or drive cycle in the regression models. This indicates that there was an underlying complexity in the data set, such that the magnitude and direction of the regression coefficient (slope) estimated for a particular fuel property varied as of function of at least one of these categorical variables. It was also noted that while the oxygenate content was not a regression parameter in the statistical analysis some of the underlying fuel property impacts attributed to distillation properties may in fact be due to the presence of oxygenates.

[4] T10, T50, T70, and T90, respectively, represent the temperatures at which 10%, 50%, 70%, and 90% of a fuel by volume boils off during a ASTM D-86 test, while EP represents the maximum temperature achieved during a ASTM D-86 test when the fuel is essentially entirely vaporized.

[5] Particulate Matter Index (PMI), calculated based on the vapor pressure and Double Bond Equivalent (DBE) of fuel components. (Aikawa et al 201, 2013)

3.2 Key findings from Annex 54

Following the organization of the results in Section 2, the key findings in the studies reported to Annex 54 can be summarized as follows:

Fundamentals of combustion and pollutant formation in a GDI Engine

- The high-speed visualization fuel-air mixing and sooting combustion in an optically accessible single cylinder engine (Germany) offers an effective technique to evaluate general trends and tendencies of soot formation in GDI engines.

- Catalyst heating operating conditions are critical as they strongly contribute to overall soot emissions in driving cycles. At these operating conditions E20 exhibits a higher sooting tendency as compared to isooctane.

- High speed visualization observations show that soot was formed in fuel rich regions with incomplete evaporation of fuel droplets remaining from the injection event.

- The evaporation process of E20 fuel spray and mixing behavior is different from that of isooctane, showing a more compact rich mixture cloud with surrounding lean areas near the spark plug region constituting a significant source of soot formation.

Effect of Alcohol Fuel Blends on Emissions from GDI Vehicles

- In the two studies (Chile and Israel) reviewed for Annex 54, alcohol blends generally had favorable effects on regulated gaseous emissions, the effect being stronger with higher percentage of alcohol in the fuel blend.

- Direct and indirect observations in two studies (via tailpipe measurements in the Israel study, secondary formation in the smog chamber in the Chile study) suggest a favorable effect on PM emissions with alcohol fuel blends, particularly in the case of GDI vehicles. However, in the single cylinder study (Germany) PM in exhaust increased with increased alcohol content likely due to the formation of fuel-rich zones during compression.

- Minor effects of alcohol content (E21 and iBu12) on PM emissions were observed in the Unites States study on start-stop operation, although these were not consistent in all cases on whether the effect was positive or negative.

Effect of Start-Stop Operation on Emissions from GDI Vehicles

- For the GDI vehicle studied (United States) PM emissions in the early part and accelerations in cold started driving cycles dominated the PM emissions for both start-stop and no start-stop operation of a GDI vehicle.

- The difference in PM mass emissions was not very large between start-stop and no start-stop operation over the hot started FTP driving cycle, suggesting that the additional starts are unlikely to significantly increase the PM emissions. If this vehicle is representative of the market, this finding is important as GDI engines penetrate the light-duty market and more manufacturers adopt start-stop for fuel economy

Effect of Gasoline Particulate Filters on Emissions from GDI Vehicles

- The gasoline particulate filters studied with GDI engines in two studies (Canada and Switzerland) were generally effective in reducing PM emissions quantified by mass or number of particles emitted per distance travelled. Some of these results showed PN emissions that could meet the regulatory limit of 6 x 10e11 particles/km.

- In the Canada study some effect of GPF on gaseous emissions were noticed although these were attributable to the fact that the retrofit GPF had replaced part of the OEM catalyst on the vehicles.

- In the Switzerland study the effect of GPF on secondary aerosol formation and genotoxic emissions were also addressed as discussed below.

Secondary Organic Aerosol Formation Potential of Emissions from GDI Vehicles

- In the Chile study observations on the progress of photochemical reactions in a smog chamber filled with dilute exhaust suggested that the rate of pollutant formation (gaseous and PM) was slower with increased alcohol content in the fuel used, suggesting that the use of higher ethanol blends may have a positive impact on air quality.

- In the Switzerland study, it was observed that while GPFs remove elemental black carbon particles, the volatile components of primary organic aerosol are not significantly reduced, thus SOA formation was not affected by the tested GPFs. It was suggested that future work on "4-way" catalysts should be conducted to understand whether reductions of SOA precursors, SOA production, and semi-volatile primary PM can also be achieved.

Genotoxicity of Emissions from GDI Vehicles

- In the Switzerland study, the emissions of 4- to 5-ring PAH compounds from most GDI vehicles exceeded those of the benchmark diesel vehicle, whereas those of the less volatile 6- and 7-ring PAHs were comparable to the emissions of the diesel vehicle.

- Using the toxicity equivalents approach for the eight PAH compounds, the genotoxic potential of the emissions from GDI vehicles were compared with the benchmark diesel vehicle equipped with a particle filter in the cold-started WLTC. In all cases the GDI vehicles released more PAHs than the benchmark diesel vehicle.

- The effect of ethanol blending on genotoxic emissions for a GDI vehicle was studied with one Euro-5 GDI vehicle, Looking at the combined genotoxic potential of the eight carcinogenic PAH compounds ethanol blending gave substantial reductions, most pronounced in the hot WLTC with reductions of 77% and 84% for E10 and E85 respectively.

- Two catalyst coated GPFs lowered emissions of genotoxic PAHs while another, non-catalyst GPF had more PAH after the filter than before. It was noted that fully integrated catalytic GPFs, operated at higher temperatures, allowing the combustion of accumulated soot and adsorbates, will be needed to lower the genotoxic potential of GDI vehicle exhausts to levels already achieved for diesel vehicles.

References

AFHB 2016. **EmGasCars** Research of Nanoparticles and of Non-Legislated Emissions from GDI Cars, J. Czerwinski, P. Comte, Y. Zimmerli, Abgasprüfstelle und Motorenlabor (AFHB) Final Report. Swiss Federal Office of Energy.

Aikawa, K., Sakurai, T., and Jetter, J., "Development of a Predictive Model for Gasoline Vehicle Particulate Matter Emissions," SAE Technical Paper 2010-01-2115, 2010,

Aikawa, K. and Jetter, J.J., "Impact of Gasoline Composition on Particulate Matter Emissions from a Direct-Injection Gasoline Engine: Applicability of the Particulate Matter Index," International J of Engine Research 15(3):298-306, 2013.

Czerwinski, J., Comte, P., Heeb, N., Mayer, A. et al., "Nanoparticle Emissions of DI Gasoline Cars with/without GPF," SAE Technical Paper 2017-01-1004, 2017

Czerwinski, J., Comte, P., Stepien, Z., and Oleksiak, S., "Effects of Ethanol Blend Fuels E10 and E85 on the Non-Legislated Emissions of a Flex Fuel Passenger Car," SAE Technical Paper 2016-01-0977, 2016

Empa, 2017. **GASOMEP**: Current Status and New Concepts of **Gas**oline Vehicle Emission Control for **O**rganic, **Me**tallic and **P**articulate Non-Legislative Pollutants. P. Comte, J. Czerwinski, A. Keller, N. Kumar, M. Muñoz, S. Pieber, A. Prévôt, A. Wichser, N. Heeb, Final Scientific report of the CCEM-Mobility project 807, Swiss Federal Laboratories for Materials Science and Technology

Araji, F. and Stokes, J., "Evaluation of Emissions from Light Duty Trucks with and without the Use of a Gasoline ParticulateFilter," SAE Technical Paper 2019-01-0971, 2019

Frenzel I, Krause H, Trimis D. Study on the influence of ethanol and butanol addition on soot formation in iso-octane flames. Energy Procedia 120 (2017) 721-728

Gramsch, E., V. Papapostolou, F. Reyes, Y. Vásquez, M. Castillo, P. Oyola, G. López, A. Cádiz, S. Ferguson, M. Wolfson, J. Lawrence & P. Koutrakis . Variability in the primary emissions and secondary gas and particle formation from vehicles using bioethanol mixtures, Journal of the Air & Waste Management Association, 68:4, 329-346, 2018

IARC (International Agency for Research on Cancer). **Some non-heterocyclic polycyclic aromatic hydrocarbons and some related exposures**, Monogr Eval Carcinog Risks Hum, 92(2010), pp. 765-771.

IEA-AMF 2015. "Particulate Measurements: Ethanol and Isobutanol in Direct Injection Spark Ignited Vehicles", Debbie Rosenblatt, Christine Morgan, Steve McConnell, Jukka Nuottimäki, A Report from the IEA Advanced Motor Fuels Implementing Agreement, Annex 35-2, January 2015.

Karavalakis, G., Durbin, T.D., Yang, J., Ventura, L. et al., "Fuel Effects on PM Emissions from Different Vehicle/Engine Configurations: A Literature Review," SAE Technical Paper 2018-01-0349, 2018

Koegl M, Hofbeck B, Will S, Zigan L. Investigation of soot formation and oxidation of ethanol and butanol fuel blends in a DISI engine at different EGR-rates. Applied Energy 209 (2018) 426-434

Koegl M, Hofbeck B, Will S, Zigan L. Influence of EGR and ethanol blending on soot formation in a DISI Engine. Proceedings of the Combustion Institute 37 (2019) 4965–4972

Munoz M., Heeb N. V., Haag R., Honegger P., Zeyer K., Mohn J., Comte P., Czerwinski J. " Bioethanol blending reduces nanoparticle, PAH and alkyl- and nitro-PAH emissions and the genotoxic potential of exhaust from a gasoline-direct injection flex-fuel vehicle", Environ. Sci. Techn., 60, 11853-11861, 2016.

Petry, T.; Schmid, P.; Schlatter, C. The use of toxic equivalency factors in assessing occupational and environmental health risk associated with exposure to airborne mixtures of polycyclic aromatic hydrocarbons (PAHs) *Chemosphere*, 32 (4) 639- 648, 1996.

Pieber, Simone M., Nivedita K. Kumar, Felix Klein, Pierre Comte, Deepika Bhattu, Josef Dommen, Emily A. Bruns, Doğuşhan Kılıç, Imad El Haddad , Alejandro Keller, Jan Czerwinski, Norbert Heeb, Urs Baltensperger, Jay G. Slowik, and André S. H. Prévôt, Gas-phase composition and secondary organic aerosol formation from standard and particle filter-retrofitted gasoline direct injection vehicles investigated in a batch and flow reactor, Atmos. Chem. Phys., 18, 9929–9954, 2018

Raza, M., L. Chen, F. Leach and S. Ding, "A Review of Particulate Number (PN) Emissions from Gasoline Direct Injection (GDI) Engines and Their Control Techniques," *Energies,* vol. 11, no. 6, 2018.

Storch M, Lind S, Will S, Zigan L. Influence of ethanol admixture on the determination of equivalence ratios in DISI engines by laser-induced fluorescence. Applied Optics 55 (2016) 8532-40.

Storch, M., Florian Hinrichsen, Michael Wensing, Stefan Will, Lars Zigan, (2015). The effect of ethanol blending on mixture formation, combustion and soot emission studied in an optical DISI engine. Applied Energy 156 (2015) 783–792

Storch M, Zigan L, Wensing M, Will S. Systematic Investigation of the Influence of Ethanol Blending on Sooting Combustion in DISI Engines Using High-Speed Imaging and LII. SAE Technical Paper 2014-01-2617

Storey, J.M., Moses-DeBusk, M., Huff, S., Thomas, J. et al., "Characterization of GDI PM during Vehicle Start-Stop Operation," SAE Technical Paper 2019-01-0050, 2019.

U.S. Environmental Protection Agency. 2018. "Light-Duty Automotive Technology, Carbon Dioxide Emissions, and Fuel Economy Trends: 1975 Through 2017." Annual Report EPA-420-R-18-001. Washington, DC: U.S. Environmental Protection Agency.
https://www.epa.gov/sites/production/files/2018- 01/documents/420r18001.pdf

U.S. EPA Priority Pollutant List, December 2014
https://www.epa.gov/sites/production/files/2015-09/documents/priority-pollutant-list-epa.pdf (Accessed 3 December 2018)

Yang, J., Patrick Roth, Thomas D. Durbin, Kent C. Johnson, David R. Cocker, III, Akua Asa-Awuku, Rasto Brezny, Michael Geller, and Georgios Karavalakis, Gasoline Particulate Filters as an Effective Tool to Reduce Particulate and Polycyclic Aromatic Hydrocarbon Emissions from Gasoline Direct Injection (GDI) Vehicles: A Case Study with Two GDI Vehicles, Environ. Sci. Technol. 2018, 52, 3275–3284.

Annex A: Report from Germany

Report for Annex 54 GDI and Alcohol Fuels

LTT Erlangen, FAU, Germany

Summary

The studies conducted at Institute of Engineering Thermodynamics (LTT, Friedrich-Alexander-Universität Erlangen-Nürnberg (FAU), Germany) contain fundamental investigations of mixture formation and soot formation in an optically accessible GDI engine using laser-based diagnostics. Further characterizations of PM are conducted in the exhaust gas duct of a metal GDI engine equipped with a GPF. Different ethanol-gasoline mixtures (e.g. E20, E40, E85) and other model fuel-mixtures (including iso-octane and toluene) as well as butanol mixtures (e.g. B20) are studied in a wide range of operating points.

1 Project description

These results were generated in the framework of the interdisciplinary Junior Research Group "BiOtto - Formation of soot particles and catalytic filter regeneration for application of biomass fuels in direct-injection spark-ignition engines" (Main applicant: Dr. L. Zigan), which was funded by the German Federal Ministry of Food and Agriculture (BMEL) through the Agency for Renewable Resources (FNR), FKZ: 22026711. The junior research group consisted of four sub-projects and further involved project partners are Prof. Michael Wensing (LTT) at FAU, Prof. C. Hasse (STFS, TU Darmstadt), Prof. S. Kureti (RT) at TU BA Freiberg and Prof. D. Trimis (Engler-Bunte-Institute (ebi), Division of Combustion Technology of Karlsruhe Institute of Technology (KIT)). An overview of the project structure is given in Figure 1.

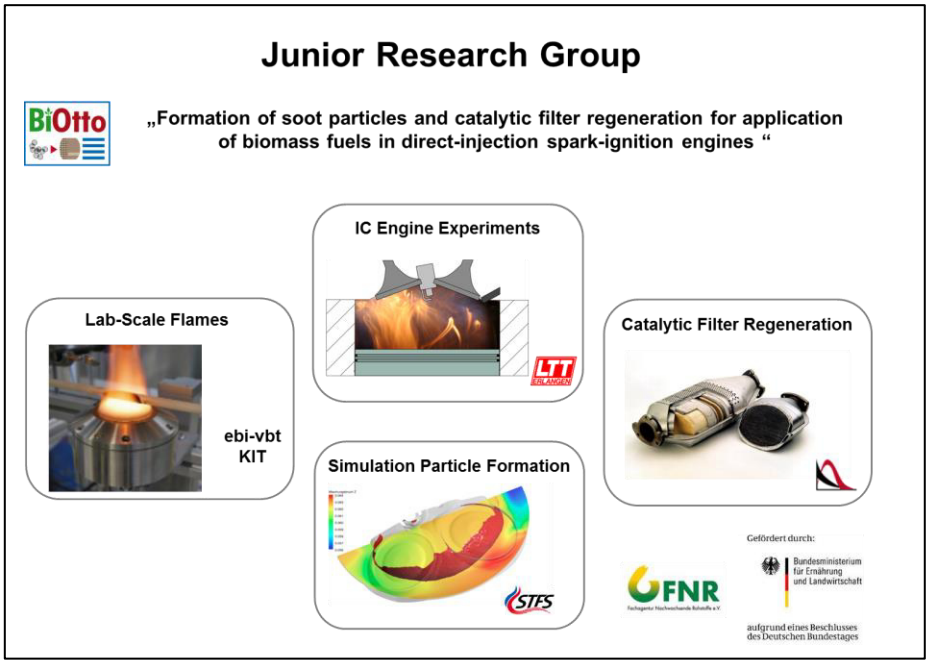

Figure 1: Structure of the Junior Research Group "BiOtto" and involved sub-project partners.

The soot formation and oxidation was examined in detail for gasoline fuels with variable biofuel content (ethanol and butanol). For a fundamental understanding of the potentials and limitations of future fuel blends with respect to soot emissions, laser-based measurement techniques were utilized in a partially transparent engine with direct injection at LTT Erlangen. Furthermore, IC engine simulations of soot formation and oxidation were conducted at STFS TU Darmstadt for different biofuel mixtures. Fundamental studies in laminar flames were conducted at ebi vt, KIT for a basic characterization of the particle formation and for its modelling and validation. The simulation results and experimental data delivered the boundary conditions for the knowledge-based development of a highly efficient catalyst for the rapid oxidation of soot in particle filters (conducted at RT, TU BA Freiberg). The resulting integrated module consists of a particle filter and a three-way catalyst. The catalytic particle filter developed at RT was tested and evaluated in a metal engine at LTT Erlangen. The work at LTT was focused on the mechanisms of sooting combustion in IC engines with gasoline direct injection. In addition to the IC engine measurements, additional studies were carried out in the injection chamber in order to identify spray-induced soot formation. For this purpose, the individual processes of atomization, evaporation and sooting combustion are investigated using laser-based methods and high-speed measurements of soot luminescence. These preliminary investigations also served for selection of relevant operating points with increased sooting combustion and fuel mixtures for measurements in the transparent IC engine. These results can be found in references [1-5] and are not described here.

In order to evaluate soot formation and soot oxidation in the optically accessible IC engine, mixture formation analysis were conducted as well as soot distribution measurements using soot luminescence and light extinction measurements (see also references [6-10]. Additionally, exhaust gas measurements using an optical LII soot sensor (LII - laser-induced incandescence) were performed. At ebi (KIT) measurements were conducted in simplified model flames on a laboratory scale (see e.g. reference [11]). Here, the fuel-specific, chemical effects of soot formation can be decoupled from physical effects that occur especially in the engine because of the injection process. These flame studies served as a basis for development of novel models to describe soot formation and oxidation at STFS (see e.g. [12,13]). The analysis of the experimental and numerical results provide a deep understanding of particle formation and oxidation for utilization of biofuel blends. Furthermore, critical operating points and fuel blends can be identified, which lead to high concentration of soot, and an optimization of the injection and ignition strategy can be derived. In the subsequent sections, only the IC engine lab work is described.

2 Results

2.1 Investigations in the optically accessible IC engine

The measurements were performed in an optically accessible single cylinder engine based on a modified BMW/PSA series-production engine (“Prince”) with direct injection. The engine is equipped with a variable valve train and lateral position of the injector (BOSCH, solenoid, 7-hole). The displacement volume is 399 cm^3. The investigated operating points represent part load conditions at different injection timings (i.e. different start of injection (SOI)). Characteristic engine operating points were selected, which represent typical driving situations in order to study fuel effects and mechanisms of soot formation. The specifications of the investigated operating points are presented in Table 1.

Table 2: Specifications of the studied operating points for iso-octane.

Operating Point	unit	Base Point	Late Injection	Globally fuel rich	Catalyst heating: Inhomogeneous mixture	Catalyst heating: poolfire
Engine speed	U/min	1500	1500	1500	1200	1200
Air mass flow	kg/h	6.3	6.5	6.3	4.8	5.5
Global air fuel ratio λ	-	1	1	0.75	1	1
IMEP	bar	2.7	1.2	2.6	1.8	2.2
Rail pressure	bar	70	70	70	70	70
Injection time (SOI1/SOI2)	°CA bTDC	300/-	145/-	300/-	300/73	300/50
Injection duration (SOI1/SOI2)	ms	1.25	1.2	1.8	0.94/0.24	0.78/0.48
Spark timing	°CA bTDC	28	28	28	0	0

It should be noted that only few operating points are shown here and significantly more parameter variations were carried out (for example variation of injection timings, injection duration etc.), which can also be used to optimize the combustion process for the biofuel mixtures.

The “Base Point” refers to an early fuel injection leading to a homogeneous stoichiometric fuel-air mixture. Similar IC engine parameters were used for the Operating Point “Globally fuel rich mixture”, mainly the global relative air-fuel ratio (λ) was adjusted to 0.75 (or an equivalence ratio ϕ of 1.33). The other operating points refer to late injections or split injections, which are usually applied for heating of the catalyst during cold start operation. For a very late second injection, the fuel wall wetting is observed leading to sooting pool fires.
The cylinder head, liner and lubricant oil were conditioned to a temperature of 333 K while the fuel temperature was kept constant at 293 K. The optical access is realized by a quartz glass window in the bottom of the piston and a quartz glass ring liner in the upper half of the cylinder (see also Figure 2). Further specifications of the IC engine and experimental setup are provided in references [7,8]. Usually, iso-octane was used as surrogate fuel, which was necessary for the modelling study (at STFS) and the investigation of lab flames (ebi). Iso-octane was also chosen as non-fluorescent base fuel in the mixture formation study (section 2.1.1). In section 2.1.3, a two-component fuel was chosen (“Toliso”, which consists of iso-octane (65 vol.%) and toluene (35 vol.%)) and in section 2.2 a multi-component gasoline fuel. In reference [4] the authors performed a comparison of these surrogate fuels to gasoline regarding the soot formation in a spray flame.

2.1.1 Mixture formation study using laser-induced Fluorescence (LIF)

Planar laser-induced fluorescence (LIF) is used to clarify the effects of biofuel blends on mixture formation and the resulting sooting combustion. Details about the measurement technique, especially for usage of ethanol blends, can be found in reference [6]. By visualizing fuel rich zones, potential sources of soot formation can be identified and correlated with measured PM emissions. For planar LIF, a liquid tracer ("dye" or marker substance, here triethylamine, "TEA") is added to the non-fluorescent base fuel (in this study iso-octane, or ethanol/iso-octane blends, respectively). The tracer fluoresces after excitation with a laser (wavelength: 248 nm). The signal

is recorded by using an intensified CCD (ICCD) camera. The fluorescence depends on the local fuel-air mixture and can be used to determine the local equivalence ratio. The measurement technique is robust and well established for IC engine studies (see e.g. [6,7,17] and references therein). Figure 2 shows the intersection of two laser light sheets in the optically accessible cylinder and the resulting field of view with an example of the fuel-air ratio distribution (in terms of the equivalence ratio ϕ). One light sheet is coupled through the quartz glass liner and the other one enters the cylinder through the piston window.

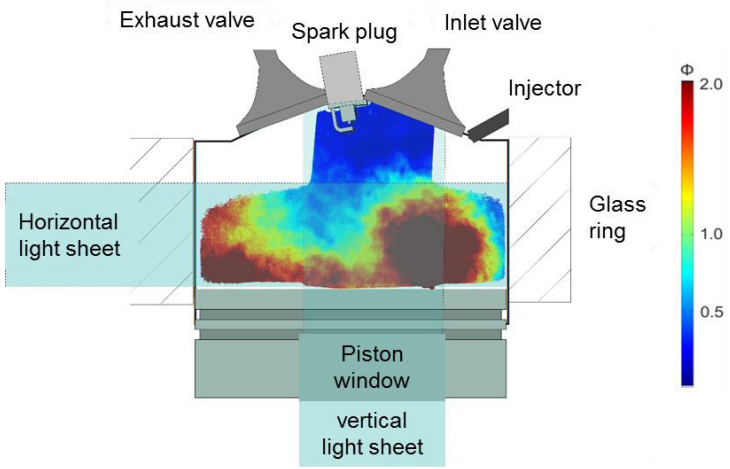

Figure 2: Optically accessible IC engine cylinder with horizontal and vertical laser light sheet. The camera field of view contains an example image of the mixture formation (FAR, ϕ) obtained by overlapping two laser light sheets.

In Figure 3 the mixture distribution is presented for the operating point “Late injection” for the fuels iso-octane, E20, E85 and pure ethanol. For the time point 108°CA before TDC (left column), no quantification of the mixture in the vapor phase is possible because there is still a large amount of the liquid fuel present, which falsifies the fluorescence signal. Furthermore, the fuel itself (i.e. the ethanol content) has a great influence on the fluorescence signal of the liquid phase, see the discussion in reference [6]. Overall, the mixture distribution for all fuels at later times appears very similar in structure. Very fuel-rich zones are visible near the piston and a "tumble flow" is formed during compression, so that a larger vortex with a fuel-rich mixture is transported towards the spark plug. At later points in time, this mixture stratification is reduced, while larger inhomogeneities and richer zones exist esp. for iso-octane and E20 (see for example 48°CA). These locally fuel-rich zones of E20 and iso-octane can explain the significantly larger PM concentration in the exhaust gas for these two fuels compared to E85 and pure ethanol (see Figure 4). In these fuel-rich zones, sooting combustion was also identified in soot luminescence measurements [8]. Further details of the mixture formation study can be found in references [6,7] also for further operating points.

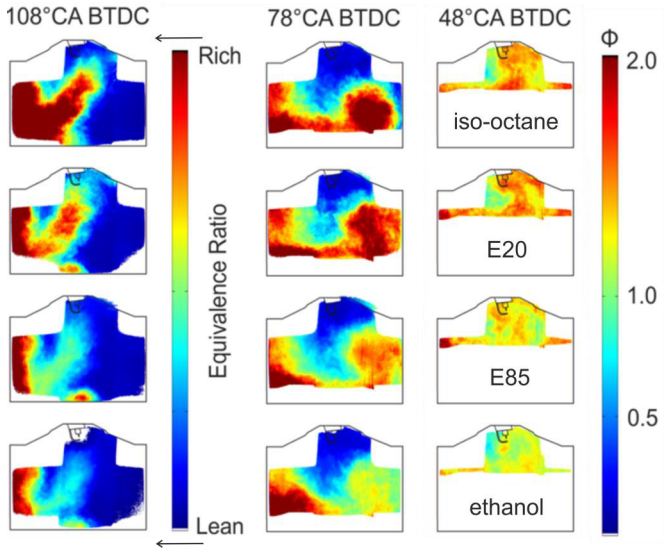

Figure 3: Distribution of fuel-air ratio for OP "Late injection" for iso-octane (top row), E20 (row 2), E85 (row 3) and pure ethanol (bottom row) (following reference [6], in which more results are listed).

2.1.2 Results of measurements conducted in the exhaust gas of the optically accessible engine

Measurement of soot concentrations for ethanol blends

Measurements were conducted in the exhaust gas system of the optically accessible IC engine. For the measurements, an optical soot sensor was applied, which has been developed at LTT. The LII soot sensor (LI²SA) is based on the principle of laser-induced incandescence (LII). Soot particles are heated by a laser, evaporated and thereby excited to radiate. The signal intensity of radiation is a measure of the concentration of carbon particles. The measuring range of the sensor is between 0.001 and 200 mg/m³ [14]. The sensor was implemented directly in the exhaust system. The IC engine was operated for 90 s for each OP and fuel. From the resulting signal curve, the median of the particle concentration was then formed. Figure 4 shows a comparison of the measured average particle concentration for the investigated operating points for the fuels ethanol, E85, E20 and iso-octane.

For all operating points it can be seen that the particle concentration is largest for E20 and iso-octane. The highest particle concentrations were measured for the operating points "Globally rich mixture" and "Catalyst Heating: Poolfire". Furthermore, the fuel-dependent results of the soot radiation (see also reference [8]) and light extinction measurements (see section 2.1.3) in the cylinder can be correlated with the trends of the particle concentrations in the exhaust gas.

For the "Base point" and for the "late injection", the soot concentrations for E20 and iso-octane are comparable. Furthermore, similar trends of soot concentration for E20 and iso-octane were found in laboratory flames [11]. There, for iso-octane and low ethanol concentrations at λ = const., a very similar particle size distribution and particle number as has been found, especially under engine relevant short residence times. In these premixed laboratory flames, however, only the influence of chemical fuel properties (such as the O/C ratio) is present.

The operating point "catalyst heating: inhomogeneous mixture" shows the highest particle concentration for E20, which cannot be explained by the effect of the chemical fuel properties on the formation of soot particles. This trend is also evident for further catalyst heating points, see operating point "Catalyst heating: Inhomogeneous

mixture + poolfire". In this case, partial piston wetting occurs during the second injection, so that generally higher particle concentrations result. It becomes clear that the soot emission not always decreases with increasing admixture of ethanol. Especially for lower ethanol admixtures, in some cases significantly higher soot particle concentrations can occur for E20 in comparison to the base fuel. This suggests that under certain operating conditions (e.g., short available evaporation and mixing times and high combustion chamber pressure), the importance of physical fuel properties dominates soot formation and chemical properties play a minor role. This effect was also visible in the mixture formation analysis using laser-induced fluorescence (see section 2.1.1) and is further analysed in light extinction measurements (see section 2.1.3).

Noteworthy is also the operating point "late injection", which shows no significant increase in the soot concentration in the exhaust gas compared to the base point. Although the global air ratio was set to stoichiometric conditions, locally fuel rich zones are expected that should lead to stronger sooting combustion. This indicates that soot oxidation could play a dominant role. The role of in-cylinder soot oxidation must also be analysed in more detail specifically for ethanol mixtures (see section 2.1.3).

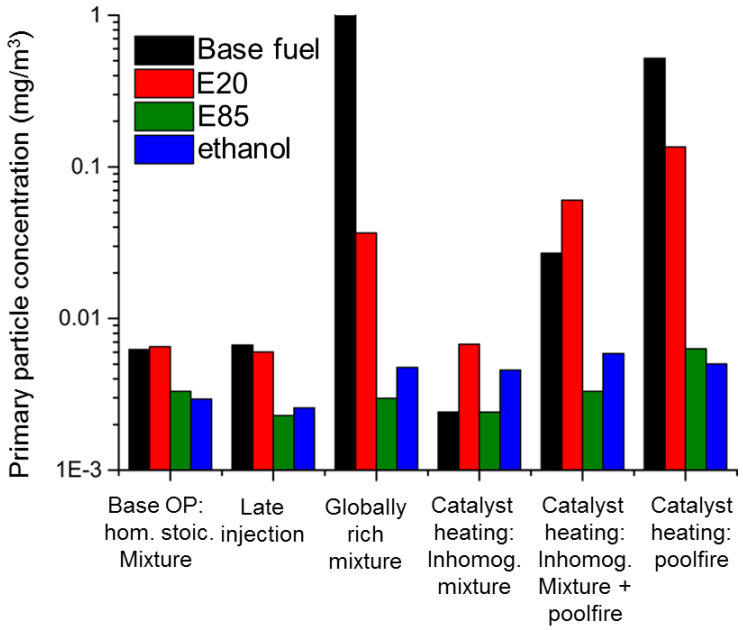

Figure 4: Particulate concentration in exhaust gas for a selection of the investigated operating points and the fuels iso-octane (base fuel), E20, E85 and pure ethanol, measured with the LII exhaust gas sensor. Parts of the data are extracted from reference [8].

Measurement of soot concentrations for butanol

In the following, the influence of pure butanol on the formation of soot is presented. Figure 5 shows a comparison of the measured average particle concentration for the previously defined operating points for the pure substances iso-octane, ethanol and n-butanol.
For the operating points "base point", "late injection" and "global rich mixture", the exhaust particle emissions of butanol behave similarly to those of ethanol. For butanol, chemical mechanisms (due to the fuel-bound oxygen content) also seem to dominate soot formation for these operating points. Under the "catalyst heating" operating points, a significantly increased particle concentration was detected for butanol. Physical properties of the fuel (e.g. viscosity, enthalpy of vaporization) appear to be the main factor influencing soot formation under these conditions. These properties determine atomization and evaporation and could contribute to wall wetting as well, which is further examined in further studies with relevant butanol mixtures (e.g. B20) in section 2.1.3.

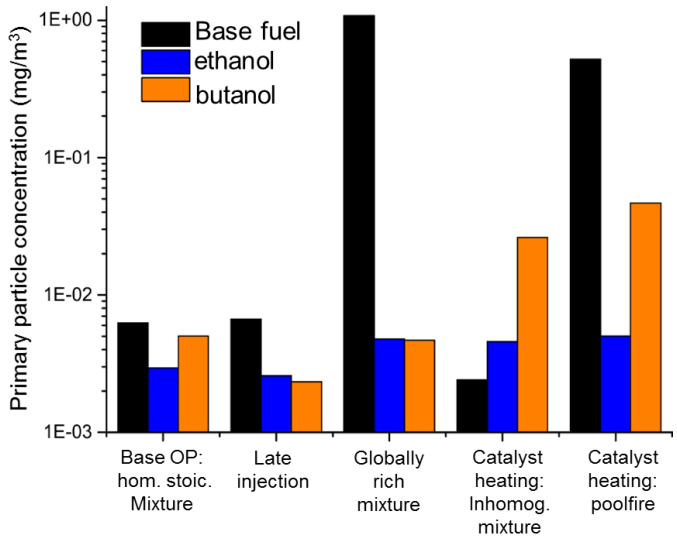

Figure 5: Particle concentration in the exhaust gas for a selection of the investigated operating points and pure substances iso-octane (base fuel), ethanol and n-butanol measured with the LII exhaust gas sensor.

2.1.3 Volumetric light extinction measurement in the optically accessible engine

The optical investigations on soot formation and oxidation were carried out in the cylinder of the above mentioned "Prince" transparent engine. Soot volume fraction measurements were conducted based on the light extinction measurement technique (LEM). The optical test setup consists of a high-speed CMOS camera (Phantom V1210, Vision Research) and a LED panel for illumination of the soot cloud. In principle, the time-resolved detection of soot radiation as well as the light extinction is possible by using a stereoscope with two different filters. The experimental setup is shown schematically in Figure 6.

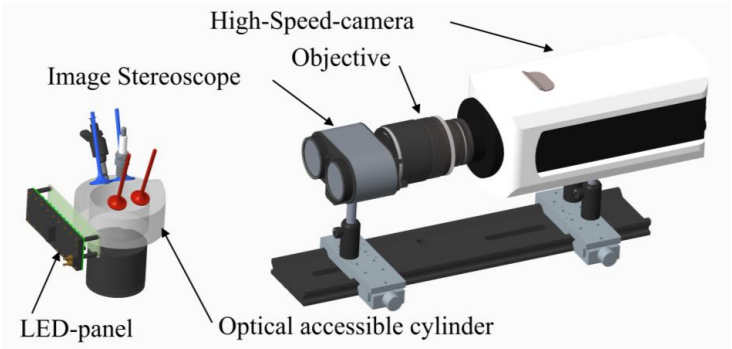

Figure 6: Optical setup for combined high-speed light extinction and soot luminescence measurements (not to scale).

For the light extinction measurement, a LED panel (in-house built) with a central wavelength of 400 nm (FWHM 12 nm) is used. A lower extinction wavelength is not meaningful due to the lower quantum efficiency of the camera in that spectral range. The camera is mounted on an optical rail for the measurements, which is mechanically decoupled from the engine test bench. The characteristics of the camera used are given in ref [9]. From the point of view of the camera, the intake valves of the engine (blue) are visible on the right in the images, the exhaust valves (red) on the left in the images. The extinction images (Figure 7, left image, a 400 nm (FWHM 25 nm) bandpass filter was used) show the light attenuation in the soot clouds. The signal of the soot

luminescence (Figure 7, right image, 650 nm long pass filter) is shown inverted for better comparison of the results with the extinction measurements.

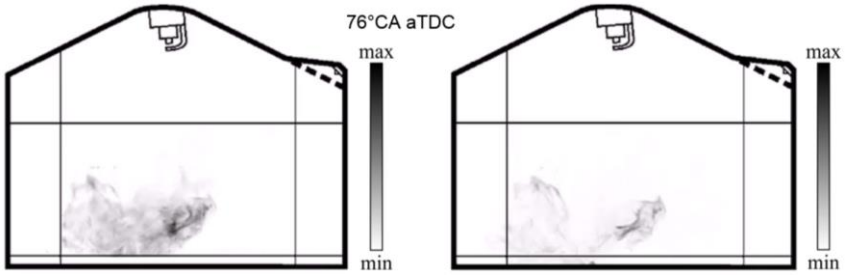

Figure 7: Examples of simultaneously recorded single shot images of light extinction at soot particles (left, using a 400 nm bandpass filter) and of soot luminescence (right, using a 560 nm long pass filter) of OP1. A high-speed camera was used in combination with a stereoscope and respective optical filters.

In Figure 7, the results of both techniques are compared for an operating point with piston wetting leading to strong sooting combustion (OP1, see definition below). The comparison of the individual images shows that the shape of the soot clouds agrees very well for both techniques. The produced soot cloud is distributed throughout the cylinder and cools down continuously. Already at 76° CA aTDC the soot has cooled down so that the signal of soot radiation gets much weaker than the light extinction signal. Thus, only the light extinction method is used for further quantitative analysis. Further data for comparison of both techniques is available in reference [9].

The operating points are similar to the ones defined above. Operating point 1 (OP1) represents early injection timing (SOI is at 300°CA bTDC), but in this case accompanied by piston wetting. OP2 represents late injection timing (SOI is at 140 °CA bTDC) leading to distinct fuel stratification. The respective parameters are presented in Table 2. The two-component surrogate fuel “Toliso” was used as a base fuel, which contains an aromatic component (toluene) leading to a more realistic sooting behavior in comparison to iso-octane. This surrogate fuel is studied in detail in reference [4] under spray combustion conditions.

Table 3: Parameters of the studied operating points for the light extinction measurements.

OP	Engine speed (1/min)	Air mass flow (kg/h)	global air-fuel ratio λ	SOI (°CA bTDC)	Ignition angle (°CA bTDC)
OP 1	1500	6.2	0.8	300	28
OP 2	1500	6.5	0.8	140	28

The relative air-fuel ratio (λ =0.8) is kept constant for all operating points and fuel blends by adjusting the fuel quantity by the injection duration. Toliso was used as well as the mixtures E20 and E40 and B20 (with Toliso as base fuel). Additionally, conditions with increased amount of synthetic exhaust gas recirculation (EGR) were studied, but these are not reported here but can be found in references [9,10].

In Figure 8, examples of single shot images are shown for one cycle of OP2. It should be noted that not the whole volume of the cylinder is accessible. However, the soot distribution and the change in its concentration is clear from the intensity of the extinction signal. This is provided in terms of the extinction *KL*, which is the product of the path length in the probe volume *L* and the average extinction coefficient *K* (for more details, see references [9,10]).

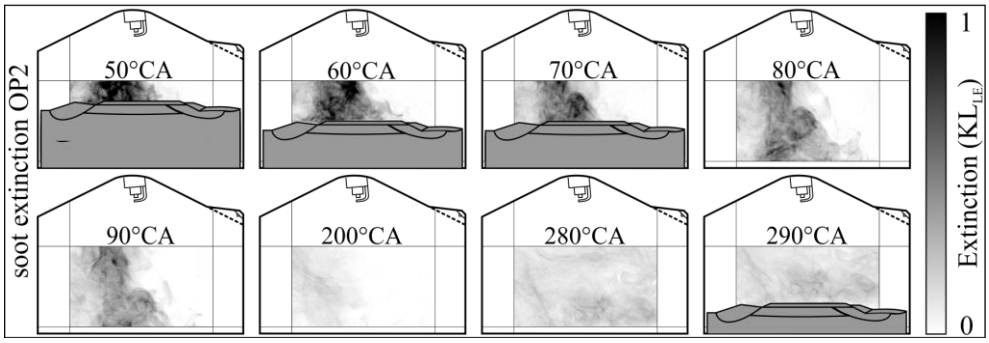

Figure 8: Examples of single shot images of light extinction in the soot particle cloud for OP2 and for E20. Measurements are extracted from reference [10], in which additional data is available.

The extinction images for OP2 also show, as for OP1, that a local soot formation occurs in the left area of the piston. The soot formation takes place here in a larger area, since in OP2 it is mainly because of the short time available for mixture formation (and less due to the piston-wetting). Still a high amount of soot can be detected at late points in time during the exhaust stroke (e.g. at 290°CA). It should be noted that the fuel-rich conditions do not lead to a complete soot oxidation and its rate can be estimated from the change of extinction, e.g. when comparing the value at 80°CA and 280°CA. At these two points in time, the piston position and the optically accessible volume of the cylinder is comparable. These points in time and the respective extinction are presented in Figure 9 for the OPs and fuel blends studied. For this quantification, 48 subsequent cycles were analysed for every OP and fuel blend.

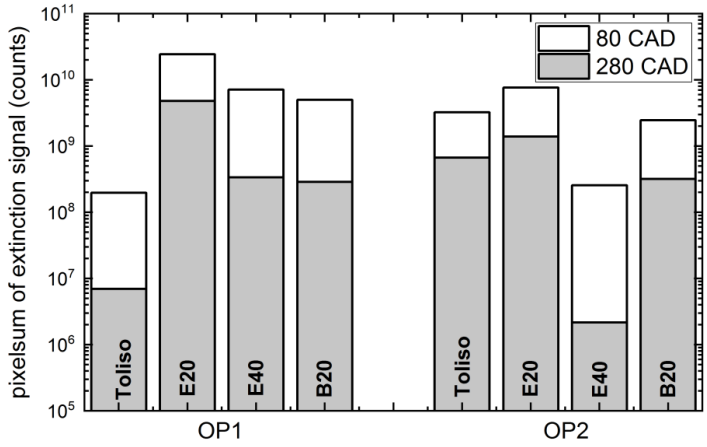

Figure 9: Accumulated averaged extinction signals (note the log-scale) at two points in time for estimation of in-cylinder soot formation and oxidation for Toliso, E20, E40 and B20; some measurements for OP1 are extracted from reference [9], in which additional data is available.

First, OP1 is analysed. Here, Toliso shows a relatively weak extinction signal and thus soot formation at 80°CA, while at 280 °CA almost all of the soot is oxidized (i.e. the extinction signal is close to the reference level). E20 shows the largest extinction and thus increased soot formation, which can be explained by the changed evaporation and mixture formation. It can be assumed that wall wetting for ethanol blends is more pronounced and that the high evaporation enthalpy of ethanol leads to an increased cooling effect in the cloud of droplets [15,16]. This higher temperature decrease in the mixture for E20 may lead to a slower vaporization and mixture formation of the remaining droplets, which contributes to sooting combustion. The larger remaining liquid fuel amount of E20 in the spray and close to the piston was also visible in the light extinction measurements conducted during injection (see [9]). Consequently, for E20 mainly physical effects contribute to the larger soot formation. Similar behaviour has been observed in LII and extinction measurements in a combusting spray studied in an injection chamber for E20 fuel blends (see reference [4]).

E40 shows similar sooting behaviour like E20 but at reduced maximum intensities. Still, the formation of soot is larger than for Toliso and higher level of soot is present in the exhaust stroke indicating more incomplete oxidation. Furthermore, also B20 shows a stronger soot formation at 80°CA compared to Toliso. Besides the higher enthalpy of vaporization mainly the large viscosity of butanol may be responsible for the stronger soot formation. This contributes to a worse atomization and evaporation and supports piston wetting. The extinction signal of E40 and B20 are comparable in the exhaust stroke (280°CA), i.e. a similar soot concentration is expected for these fuels.

In the following, OP2 is studied. In general, the same trends are found for OP2 as for OP1 for Toliso, E20 and B20, while E40 shows a much lower extinction level. Obviously, for E40 the larger amount of fuel-bound oxygen reduces the soot formation in this case and physical effects play a minor role. For Toliso, an increased soot formation was observed compared to OP1 while E20 shows a reduced extinction for OP2 compared to OP1. However, still the largest extinction levels can be determined for E20. This indicates that the physical fuel effects are more dominant for E20 compared to Toliso and E40. This is also confirmed by the slower evaporation rate of E20, which was indicated by extinction measurements during injection (see references [9,10]). B20 shows a similar soot formation and oxidation like Toliso at slightly reduced extinction levels, which is explained by the similar evaporation characteristics under these conditions. Further data of these light extinction measurements can be found in references [9,10].

2.2 Exhaust gas measurements in a 4-cylinder metal engine

The following section a turbocharged 4-cylinder metal engine with direct injection was used for studying the PM emissions of gasoline (SuperPlus, RON 98) and E20. Only E20 was chosen as biofuel blend since the previous experiments showed similar particle formation like the base fuel or even higher soot concentrations. The main purpose of this working package was the validation of the operation of a manganese oxide coated soot oxidation filter developed at RT TU BA Freiberg (these results are not reported here). For this purpose, special operating points with constant load and engine speed were chosen for soot generation and oxidation in the novel catalytic soot oxidation filter. The specifications of the IC engine are shown in table 3.

Table 3: Specifications of the 4-cylinder metal engine.

Number of cylinders / valves	4 / 4
Displacement volume (cm^3)	1801
Stroke/bore (mm)	84.1 /82.5
Effective compression ratio	9.6
Injector position	lateral
Injection system	common rail

LII measurements for determination of soot volume fraction f_v were carried out in the exhaust gas system directly after the 3-way catalyst (and in front of the catalytic soot oxidation filter). The engine management system determines the mass flows of air and fuel, as well as the relative air ratio. The engine was conditioned to 363 K at the beginning of the measurements. The temperature of the fuel and the intake air was kept constant at 294 K. The experimental engine was operated constantly at a speed of 1500 rpm. The parameters of the five operating points are given in table 4. The reference operating point OP3 serves for warm-up of the conditioned engine. In order to achieve a fast particle loading of the filter, a fuel-rich operating point (OP1) was selected at λ = 0.77. OP4 is another sooting operating point with very early injection and potential piston wetting. The parameters of the two oxidation operating points have been adjusted to achieve different exhaust gas temperatures at the filter outlet of 500°C (OP2) and 600°C (OP5), respectively.

Table 4: Operating points of the metal engine (EOI, End Of Injection).

Operating point	λ	p_{mi} (bar)	Exhaust mass flow (kg/h)	EOI (bTDC) (°CA)	comment
OP1	0.77	10.0	93.0	310	Filter loading
OP2	1.10	9.0	87.1	270	Oxidation, 500°C at filter outlet
OP3	1.00	9.5	84.7	270	reference
OP4	1.00	9.5	84.7	310	Very early injection
OP5	1.10	12.8	127.6	270	Oxidation, 600°C at filter outlet

In the following, the results of the LII soot concentration measurements are discussed, see Figure 10. All measurements were conducted for runs of 45 min. The presented data are averaged over this time and the error bars refer to temporal standard deviations. OP1 is used for filter loading and thus shows the largest mean soot volume fraction of 21 ppb. The other operating points show soot volume fractions in the range of 0.5 to 0.9 ppb. E20 shows very similar (in case of OP5) or slightly lower soot volume fractions compared to gasoline (for OP1-4). It should be noted that the metal engine has always been tested in the warm state (see above) and there is also a very good mixture homogenization because of the early injection. A late injection or split injection (which was tested in the transparent engine) cannot be realized so far. The operating points studied in the transparent engine with increased soot formation for E20 refer mainly to realistic cold start conditions and to a more inhomogeneous mixture (with fuel rich zones) and/or strong piston wetting.

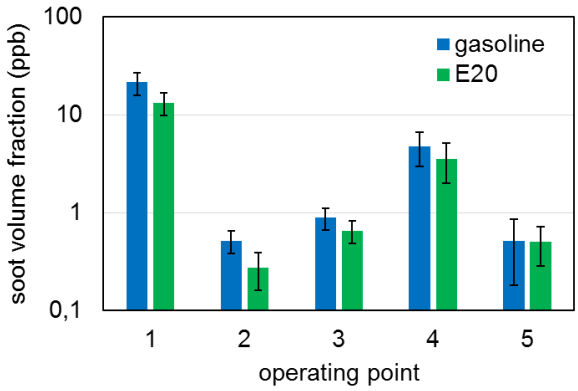

Figure 10: Time-averaged soot volume fraction and standard deviation (temporal variation) of the individual operating points for gasoline (Super Plus, RON 98) and E20. The measurements were conducted in cooperation with T. Russwurm and S. Aßmann (LTT Erlangen).

Funding

The authors gratefully acknowledge the financial support by the German Federal Ministry of Food and Agriculture (BMEL) through the Agency for Renewable Resources (FNR), FKZ: 22026711.

References

[1] Koegl, M, Hofbeck, B, Baderschneider, K., Mishra, M N , Huber, F J T, Berrocal, E, Will, S, Zigan, L. Analysis of LIF and Mie signals from single micrometric droplets for instantaneous droplet sizing in sprays. Optics Express 26(24) (2018) 31750-31766

[2] Koegl M, Mishra YN, Storch M, Conrad C, Berrocal E, Will S, Zigan L. Analysis of ethanol and butanol direct-injection spark-ignition sprays using two-phase structured laser illumination planar imaging droplet sizing. International Journal of Spray and Combustion Dynamics 2019 (in press), DOI: 10.1177/1756827718772496

[3] Storch M, Erdenkäufer S, Wensing M, Will S, Zigan L. The Effect of Ethanol Blending on Combustion and Soot Formation in an Optical DISI Engine Using High-Speed Imaging. Special Issue from 12th International Conference on Combustion and Energy Utilisation, 2014. Energy Procedia 66 (2015) 77-80

[4] Storch M, Koegl M, Altenhoff M, Will S, Zigan L. Investigation of soot formation of spark-ignited ethanol-blended gasoline sprays with single-and multi-component base fuels. Applied Energy 181 (2016) 278–287

[5] Storch M, Pfaffenberger A, Koegl M, Will S, Zigan L. Combustion and Sooting Behavior of Spark-Ignited Ethanol–Isooctane Sprays under Stratified Charge Conditions. Energy and Fuels 30 (7) (2016) 6080–6090

[6] Storch M, Lind S, Will S, Zigan L. Influence of ethanol admixture on the determination of equivalence ratios in DISI engines by laser-induced fluorescence. Applied Optics 55 (2016) 8532-40.

[7] Storch M, Hinrichsen F, Wensing M, Will S, Zigan L. The effect of ethanol blending on mixture formation, combustion and soot emission studied in an optical DISI engine. Applied Energy 156 (2015) 783-792

[8] Storch M, Zigan L, Wensing M, Will S. Systematic Investigation of the Influence of Ethanol Blending on Sooting Combustion in DISI Engines Using High-Speed Imaging and LII. SAE Technical Paper 2014-01-2617

[9] Koegl M, Hofbeck B, Will S, Zigan L. Investigation of soot formation and oxidation of ethanol and butanol fuel blends in a DISI engine at different EGR-rates. Applied Energy 209 (2018) 426-434

[10] Koegl M, Hofbeck B, Will S, Zigan L. Influence of EGR and ethanol blending on soot formation in a DISI Engine. Proceedings of the Combustion Institute 37 (2019) 4965–4972

[11] Frenzel I, Krause H, Trimis D. Study on the influence of ethanol and butanol addition on soot formation in iso-octane flames. Energy Procedia 120 (2017) 721-728

[12] Salenbauch S, Sirignano M, Marchisio DL, Pollack M, D'Anna A, Hasse C. Detailed particle nucleation modeling in a sooting ethylene flame using a Conditional Quadrature Method of Moments (CQMOM). Proceedings of the Combustion Institute 36 (2017) 771-779

[13] Salenbauch S, Sirignano M, Pollack M, D'Anna A, Hasse C. Detailed modeling of soot particle formation and comparison to optical diagnostics in premixed ethylene flames. Fuel 222 (2018) 287-293

[14] Schraml S, Kremer H, Sommer R, Leipertz A. LI^{2}SA: instrument of soot characterization and optimization of ultra-low emission vehicles. COMODIA; 2004.

[15] Trost J, Zigan L, Leipertz A. Quantitative vapor temperature imaging in DISI-sprays at elevated pressures and temperatures using two-line excitation laser-induced fluorescence. Proceedings of the Combustion Institute 34, 3645–3652, 2013

[16] Zigan L, Trost J, Leipertz A. Simultaneous imaging of fuel vapor mass fraction and gas-phase temperature inside gasoline sprays using two-line excitation tracer planar laser-induced fluorescence. Applied Optics 55 (6) (2016) 1453-1460

[17] Lind S, Trost J, Zigan L, Leipertz A, Will S. Application of the tracer combination TEA/acetone for multi-parameter laser-induced fluorescence measurements in IC engines with exhaust gas recirculation. Proceedings of the Combustion Institute 35, 3783–3791, 2015

Annex B: Report from Israel

Exhaust emissions of flex fuel vehicles fueled with RON95, M56, E85

Gideon Goldwine & Eran Sher

Technion – Israel Institute of Technology

This research was funded by the ministry of energy, state of Israel

Abstract

This research was done under Israeli-European cooperation between the Technion and the Joint Research Centre of the European Commission (JRC). The research was commissioned by the Ministry of energy, and is part of a national program for allocating crude oil substitutes for transportation fuel.

The main aim of this study was to conduct comparative research on emissions (regulated and unregulated) from vehicles equipped with a regular SI engine that can be fueled with high percentage ethanol gasoline mixtures (E85), these vehicles are known as flex fuel vehicles. The fuels that were tested during this research were: E85, RON95 and M56.

The experimental work was conducted at the vehicle emission laboratory (VELA) of the JRC, located in Ispra, Italy. The tests were performed using a standard facility for exhaust emission measurement that complies with the European regulation on type approval.

The results show that using oxygenated fuels can decease substantially the emissions compared to RON95. While the effect on NOx is relatively small, all the other emissions are decreasing beside Formaldehyde (which is not regulated currently in Europe). PN & PM emissions are decreased substantially especially for direct injection SI engines, this trend is relevant to current engine technology since three-way catalytic converter cannot decrease PN & PM, and therefore the usage of oxygenated fuels in such engines may have big benefit in decreasing PM & PN emissions. However, Formaldehyde emission is increased. Formaldehyde is emitted from all fuels (including RON95) but oxygenated fuels (and especially methanol) tend to emit more formaldehyde. This higher formaldehyde emission may be decreased by different calibration of the engine or usage of modified three-way catalytic converter. Formaldehyde emissions are larger for direct injection SI

engines compared to port fuel SI engines. Most of the formaldehyde is emitted while the TWC is cold with limited conversion efficiency.

Tested vehicles

- Vehicle 1 – manufactured at 2014, 77,000 km, direct injection, 2.4 liter, naturally aspirated, automatic transmission, homologated according to US standard.
- Vehicle 2 – manufactured at 2011, 106,000 km, Euro 5, direct injection, 2.0-liter, turbocharged, manual transmission.
- Vehicle 3 – manufactured at 2012, 50,000 km, Euro 5, port fuel injection, 1.6-liter, manual transmission.

All vehicles tested during 2015.

Emissions test facility

The measurements were carried out at VELA. The emissions test facility is in full compliance with the requirements set by the legislative procedure for vehicle type approval. The facility consists of a climatic chamber, a roller bench, and the equipment for emissions measurements. All tests were carried out at a temperature of 22°C ± 1°C. In order to follow the legislative driving cycles, the driver was assisted by a driver aid system.
Regulated pollutant emissions were measured in full accordance with the legislative test procedure for type approval (Type I test, UNECE Regulation 83) using a constant volume system (CVS) based on a full-flow dilution tunnel with a critical flow Venturi. For the non-legislative cycles, the same methodology was used.
Emissions were measured using the following analyzers/methodologies:

- CO: Infrared (IR) analyzer
- NOx: Chemiluminescence analyzer
- HC: Flame Ionization Detector (FID) analyzer
- Particulate Mass (PM): Particulate samples were collected according to the modified procedure developed in the framework of the Particle Measurement Program (PMP) and using a Pallflex TX40HI20 filter (one filter per cycle, no secondary filter). The mass was determined by weighing.
- Particle Number (PN): Total PN was measured using a system compliant (AVL APC) with the requirement defined in the Particulate Measurement Program (PMP) and now laid included in UNECE Regulation 83.

Fuel consumption

UNECE Regulation 101 establishes the methodology to be used to calculate the fuel consumption of vehicles by measuring exhaust emissions. The calculation is based on the carbon balance method, which requires the measured values of CO_2, CO, and

HC and knowledge of fuel composition in terms of C/H/O elemental content. In the type approval test, fuel consumption is calculated using default values for C/H/O from a typical reference fuel, but this is not appropriate when different fuel compositions are tested, especially in the case of oxygenated fuels. Therefore, data on each fuel's actual carbon, hydrogen, and oxygen contents are necessary for a correct calculation of fuel consumption. In addition, in order to calculate the energy used by the vehicle to complete the driving cycle, the heating value of each test fuel is needed. These data were calculated for the test fuels from detailed gas chromatography (GC) analyses carried out on each fuel.

The fundamental equation for the carbon balance calculation of fuel consumption is:

- $\mathbf{FC_m = (CWF_{exh} \times HC + 0.429 \times CO + 0.273 \times CO_2) / CWF_{fuel}}$ **(in g/km)**

where:

- FC_m is the calculated fuel consumption in g/km
- CWF_{exh} is the carbon mass (weight) fraction of the hydrocarbon emissions
- HC is hydrocarbon emissions in g/km
- 0.429 is the carbon mass fraction of CO
- CO is carbon monoxide emissions in g/km
- 0.273 is the carbon mass fraction of CO_2
- CO_2 is carbon dioxide emissions in g/km
- CWF_{fuel} is the carbon mass (weight) fraction of the fuel

CWF_{exh} is relatively unimportant (and very difficult to measure or calculate) because hydrocarbon emissions from modern vehicles are very low. The correct CWF_{fuel} is critical, however, so the CWF_{exh} was assumed to equal the CWF_{fuel}. Fuel consumption in l/100km could then be calculated from the following equation:

- $\mathbf{FC_{l/100km} = (FC_m \times 100) / (SG_{fuel} \times 1000)}$

where SG_{fuel} is the fuel's specific gravity in kg/liter.

The energy consumption in MJ/100km is calculated from:

- $\mathbf{EC_{MJ/100km} = FC_{l/100km} \times SG_{fuel} \times LHV_{fuel}}$

where LHV_{fuel} is the fuel's lower heating value (LHV) in MJ/kg.

Carbonyls

Carbonyls (formaldehyde) were measured with FTIR. A high-Resolution Fourier Transform Infrared spectrometer (HR-FTIR – MKS Multigas analyzer 2030,

Wilmington, MA, USA. The device is made up of a multipath cell (optical length: 5.11 m), a Michelson interferometer (spectral resolution: 0.5 cm1, spectral range: 600–3500 cm1) and a liquid nitrogen cooled mercury cadmium telluride detector (MCT). The raw exhaust was sampled directly from the tailpipe of the vehicles with a heated PTFE (politetrafluoroetilene) line and a pumping system (flow: ca. 10 L min1, T: 191 C) in order to avoid the absorption of hydrophilic compounds (i.e., NH3, NO2, carbonyls, or ethanol) in condensed water. The residence time of the undiluted exhaust gas in the heated line before the HR-FTIR measurement cell was less than 2 s. The pressure during the measurement was 1013 hPa (±20), and the temperature was set to 191 C. The calibration of the instrument was based on a factory developed multivariate model. CO, CO2 and NOx measurements from the previously described analyzers were used to check the HR-FTIR calibration model, and to synchronize the time-resolved signal.

Test vehicle preparation

According to the test protocol, the test vehicles were required to be in good mechanical condition and preferably had to have completed at least 1,000 km on the fuel recommended by the manufacturer prior to testing. These requirements were intended to ensure that the catalyst was adequately aged and the engine combustion chamber deposits had stabilized.

For all of the vehicles, the engine oil, oil filter, and air filter were changed before starting the test program. After the oil change, the oil was aged by driving a minimum of 500 km on the dynamometer. The fuel used for the oil aging was Fuel 1 from the test fuel matrix. The engine oil complied with the grade recommendations of the vehicle manufacturer.

In addition, the following operations were performed on each vehicle:

- The exhaust system of the vehicle was checked for leaks.
- The engine was checked for leaks of the gasoline/lubricant circuit.
- When necessary, additional fittings, adapters, or devices were fitted to the fuel system in order to enable complete draining of the fuel tank. In general, the draining of the tank was accomplished by means of the vehicle fuel pump.
- When possible, the engine was equipped with suitable thermocouples to monitor the lubricant and coolant temperature.

Results

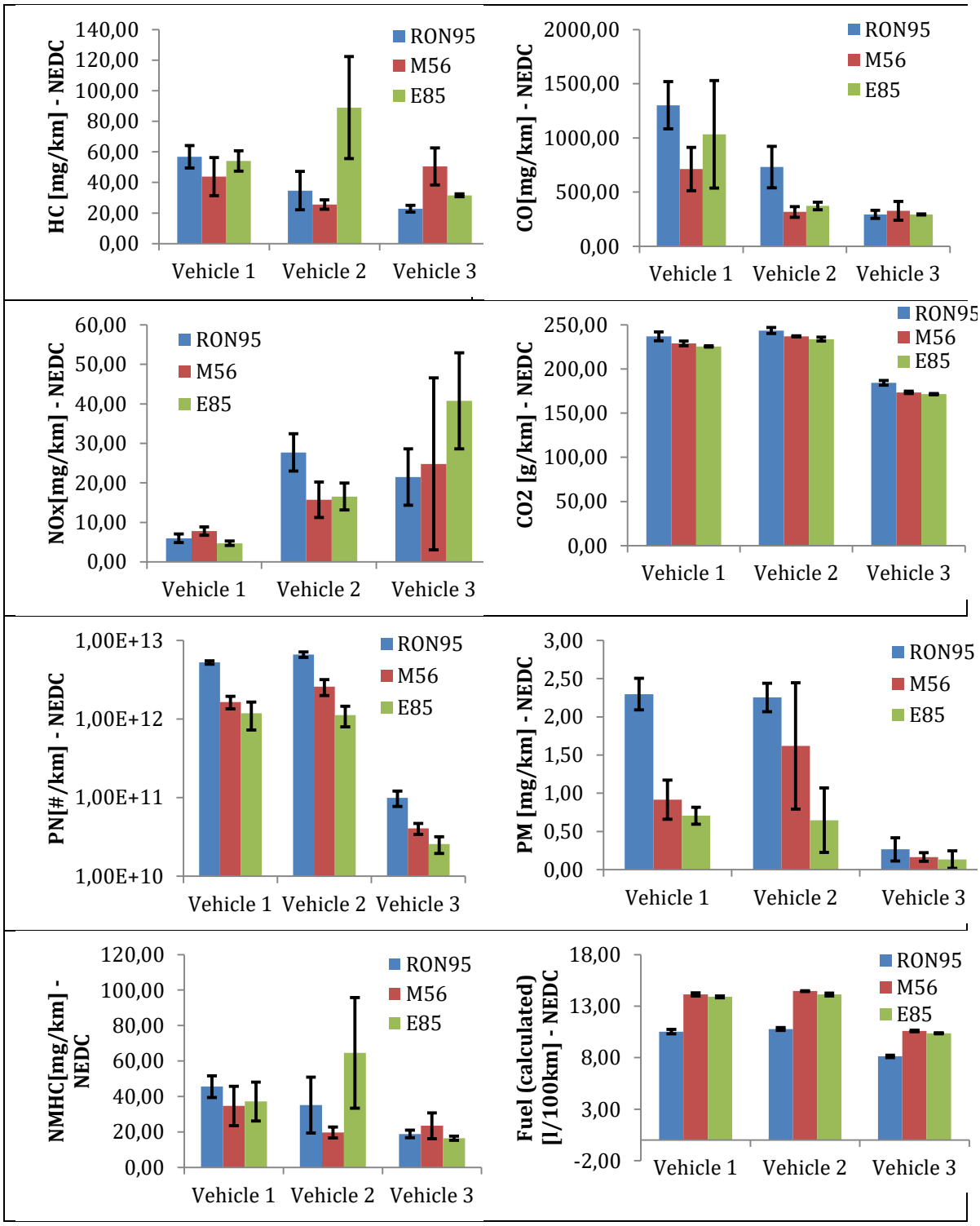
HC [mg/km] - NEDC
140,00
120,00
100,00
80,00
60,00
40,00
20,00
0,00
Vehicle 1
Vehicle 2
Vehicle 3
RON95
M56
E85
CO[mg/km] - NEDC
2000,00
1500,00
1000,00
500,00
0,00
NOx[mg/km] - NEDC
60,00
50,00
40,00
30,00
20,00
10,00
0,00
CO2 [g/km] - NEDC
250,00
200,00
150,00
100,00
50,00
0,00
PN[#/km] - NEDC
1,00E+13
1,00E+12
1,00E+11
1,00E+10
PM [mg/km] - NEDC
3,00
2,50
2,00
1,50
1,00
0,50
0,00
NMHC[mg/km] - NEDC
120,00
100,00
80,00
60,00
40,00
20,00
0,00
Fuel (calculated) [l/100km] - NEDC
18,00
13,00
8,00
3,00
-2,00

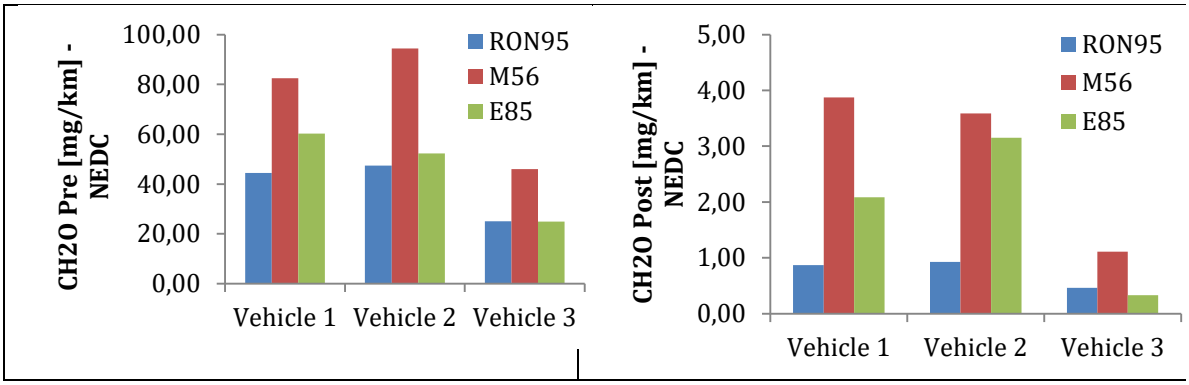

Figure 1 – Emissions for vehicle 1,2,3 during standard NEDC driving cycle.
Pre – before catalytic converter
Post – after catalytic converter
The reported results represent average of 3 independent measurements, beside for formaldehyde which stands as single measurement done by FTIR.

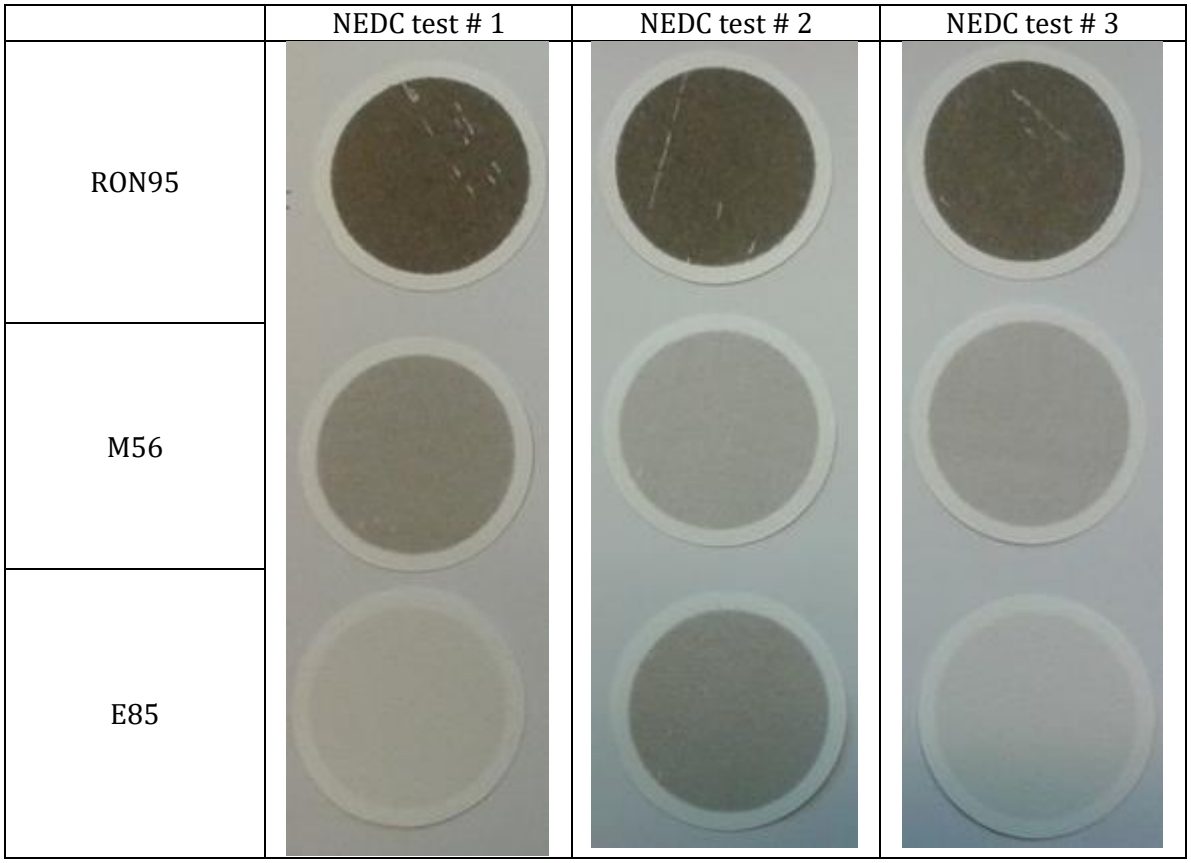

Figure 2 - PM measurements are done using standard delicate filter. These filters were collected during the measurement of vehicle number 2 and photographed. In the photograph: NEDC driving cycle, fuel 1 – RON95, fuel 2 – M56, Fuel 3 – E85. The photograph clearly shows the benefits of using oxygenated fuels compared to normal gasoline.

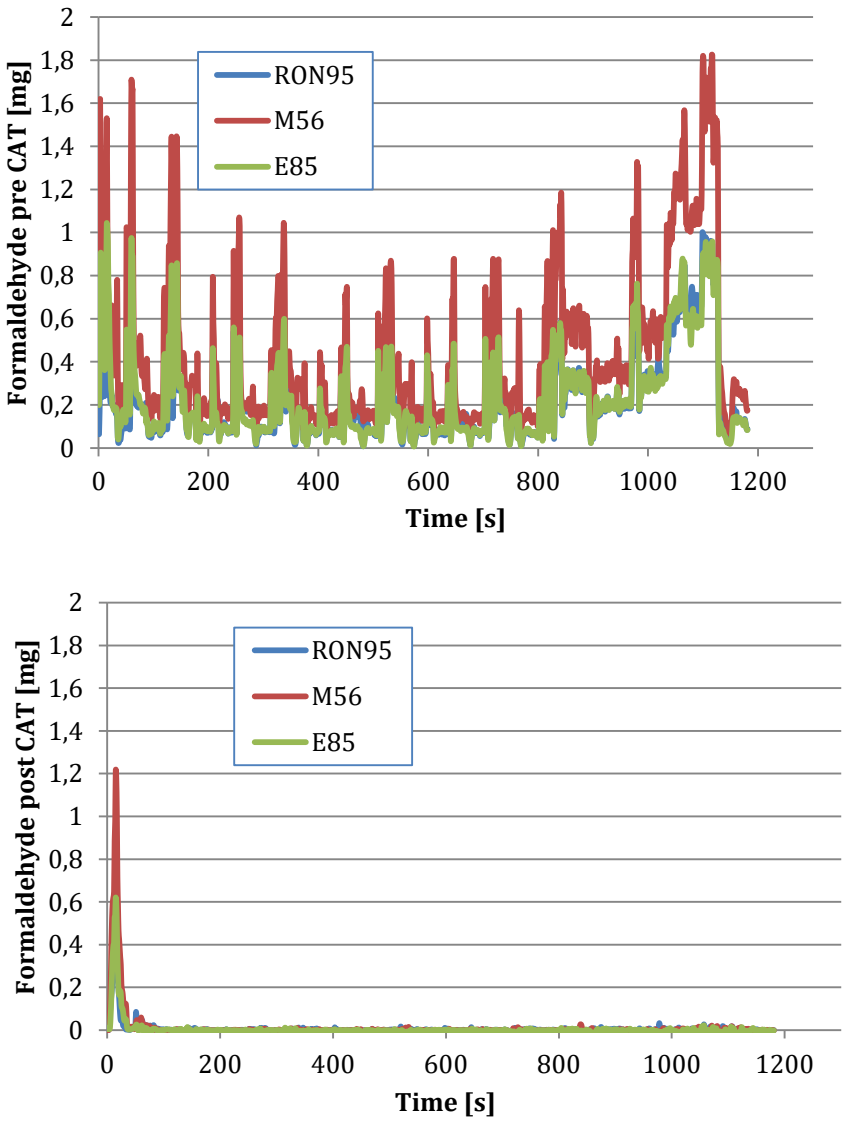

Figure 3 - The above plots are showing formaldehyde emissions during NEDC driving cycle as measured by FTIR for vehicle 2, before and after the catalytic converter.

Conclusions

Results of vehicle 1 and vehicle 2 (FFV vehicle), shows that M56 emissions compared to RON95 are lower for CO, HC and PN (4 times lower), slightly higher for NOx (but under the limit), and higher for formaldehyde (above the limit according to California air quality standards for the NEDC cycle).

Main emission of Formaldehyde is at the beginning of the driving cycle before the catalytic converter achieves light off temperature.
California emission standards for formaldehyde are stated according to FTP75 driving cycle, and therefore comparing the results which were obtained for NEDC driving cycle is not correct (FTP75 driving cycle enforces shorter heating interval for the catalytic converter). In the European legislation there is no limit of the emission of formaldehyde.
Formaldehyde was measured before and after the catalytic converter with FTIR. Formaldehyde is emitted from the combustion of all fuels, and is part of the HC emissions group. However, for M56 formaldehyde emissions from the combustion is almost doubled compared to RON95 (E85 also emits more from the combustion, but less than the M56). The catalytic converter is effectively converting the formaldehyde (efficiency of more the 95%) to carbon dioxide and water, however while the converter is cold, conversion efficiency is decreasing substantially.
From the results it seems that direct injection SI engines tend to emit more formaldehyde compared to port injection engine. Since Formaldehyde is gaseous emission it can be converted effectively in the catalytic converter, the higher emission of formaldehyde for the oxygenated fuels may be decreased by different calibration of the engine. Furthermore, a modified catalytic converter may increase the conversion efficiency of formaldehyde and decrease its emission to a level which is similar to RON95.

Vehicles 1&2 were equipped with direct injection technology (vehicle 2 was equipped also with a turbocharger), it seems that oxygenated fuels have **significant** influence over particle material emissions. For both vehicles, values of PM and PN decreased sustainably for M56 and E85 compared to RON95.
Vehicle 3 (FFV) was equipped with natural aspiration spark ignition engine, with port fuel injection system. For this kind of engine control technology particle material emissions are very low due to better evaporation of the fuel prior combustion. Also, for this vehicle M56 and E85 showed decrease emissions of PM&PN compared to RON95, but since for RON95 PM&PN values were lower also the decrease with E85&M56 was lower.
From the results it seems that direct injection SI engines tend to emit more PM/PN compared to port injection engine.

NOx emissions for all FFV vehicles were similar for all fuels, with slight decrease or increase between the different fuels.

CO emissions were lower for oxygenated fuels compared to RON95 – this trend was evident for all FFV.

HC emissions for direct injection vehicles (vehicles 1&2) was lower for the oxygenated fuels compared to RON95, however for the port fuel injected vehicle (vehicle 3) HC emissions were larger for M56 for NEDC cycle.

NMHC emissions were lower for the oxygenated fuels compared to RON95.

Carbon dioxide emission for the oxygenated fuels was lower compared to RON95. In a well calibrated engine carbon dioxide emission is anticipated to be even lower.

Overall, using oxygenated fuels (M56 & E85) has lower emissions compared to RON95. The most significant reduction was measured for PM & PN. Modern S.I engines are equipped with direct injection which increase the emission of PM & PN, the use oxygenated fuels in these engines can decrease substantially the emission of PM & PN from these engines. Emission of PM & PN from port fuel injection engines is relatively low, and while the benefit in these engines is lower (compared to direct injection engines) emission of PM & PN from port fuel injection engines is lower when oxygenated fuels are used. It is worth mentioning that in the near future S.I engines equipped with direct injection might be obliged to use particle filter in order to decrease PM & PN, the results of this research point on an alternative path – using oxygenated fuels as a measure to decrease PM & PN.